



Fabrication and characterization of poly(decylactone)  
nanoemulsions using tailor-made surfactants for  
delivery of hydrophobic drugs

Jasmin Pyrhönen

Master's thesis in Pharmacy

Pharmacy

Faculty of Science and Engineering

Åbo Akademi University

Åbo

2022

## **Abstract**

Delivery of hydrophobic drugs is a challenging field due to their poor aqueous solubility, which affects their bioavailability and pharmacological response. Nanoemulsion is a heterogeneous system of two immiscible liquids stabilized by surfactants, which has been widely utilized to enhance the aqueous solubility of drugs. Preparation of nanoemulsions using a hydrophobic oily polymer as a dispersed phase has its own advantage compared to conventional oils, such as high stability and ease of fabrication. However, the compatibility between hydrophobic drugs and polymer has a direct impact on the drug loading efficiency and thus, the aim of this work was to utilize insights obtained from molecular dynamics (MD) simulations to help predicting the miscibility of a polymeric nanoemulsion formulation with different drug molecules. The MD-calculated Hildebrand solubility parameters was used to screen for the best polymer-drug combinations. Later, the formulations were experimentally prepared to verify the simulation results. In addition, the effect of an in-house surfactant was compared with a commercially available surfactant. The MD simulation results were successfully proved in lab scale, and the use of the in-house-made surfactant in smaller quantities gave trustworthy results for a stable nanoemulsion with a high drug load.

## Table of Contents

Abstract.....	i
List of Abbreviations .....	iv
1 Introduction .....	1
1.1 Poorly soluble drugs .....	1
1.2 Nanoemulsions as dosage forms .....	2
1.2.1 Fabrication of nanoemulsions .....	3
1.2.2 Use of surfactants as stabilizers .....	4
1.2.3 Advantages of nanoemulsions.....	5
1.2.4 Challenges with nanoemulsions .....	6
1.2.4.1 Ostwald ripening and coalescence.....	7
1.3 Computational pharmaceutics - Molecular dynamics simulations .....	8
1.3.1 Application of MDS when predicting miscibility.....	9
1.3.2 Hildebrand & Hansen solubility parameter.....	10
2 Aim .....	12
3 Materials and methods.....	13
3.1 Materials .....	13
3.2 Methods .....	14
3.2.1 Selection of APIs.....	14
3.2.2 Computational assessment .....	15
3.2.2.1 Polymer modeling .....	15
3.2.2.2 Simulation system preparation .....	15
3.2.2.3 Molecular dynamics simulations .....	16

3.2.3 Synthesis of homopolymer PDL and block copolymer mPEG-b-PDL .....	18
3.2.4 Preparation of standard curves .....	19
3.2.5 Determination of aqueous solubility of pure drugs .....	19
3.2.6 Preparation of nanoemulsion.....	19
3.2.7 Characterization of nanoemulsion.....	20
3.2.7.1 Drug content .....	20
3.2.7.2 Droplet size of nanoemulsion.....	20
3.2.7.3 Nanoemulsion stability study .....	21
4 Results .....	22
4.1 Computational assessment of polymer/API bulk properties.....	22
4.2 Synthesis and characterization of PDL homopolymer and block copolymer surfactant	25
4.3 Standard curves.....	27
4.4 Aqueous solubility of pure drugs.....	30
4.5 Polymer/surfactant ratio.....	31
4.6 Characterization of nanoemulsions.....	32
4.6.1 Drug content.....	32
4.6.2 Droplet size .....	33
4.6.3 Stability .....	36
5 Discussion.....	40
6 Conclusion.....	42
7 Summary in Swedish - Svensk sammanfattning .....	43
8 References .....	45

## List of Abbreviations

<b>API</b>	active pharmaceutical ingredient
<b>DLS</b>	dynamic light scattering
<b>CED</b>	cohesive energy density
<b>CMC</b>	critical micelle concentration
<b><math>C_{Sat}</math></b>	solubilizing capacity
<b><math>D_H</math></b>	Hildebrand distance
<b><math>d</math>, nm</b>	diameter values in nanometers
<b>HLB</b>	hydrophilic-lipophilic balance
<b><math>^1H</math> NMR</b>	proton nuclear magnetic resonance
<b>HPLC</b>	high-performance liquid chromatography
<b>MD</b>	molecular dynamics
<b>MDS</b>	molecular dynamics simulation
<b>mPEG-b-PDL</b>	(methoxy-poly(ethylene glycol)-b-poly(decylactone))
<b>NTP</b>	isothermal-isobaric ensemble (a statistical mechanical ensemble where number of particles $N$ , temperature $T$ and pressure $P$ are kept constant)
<b>O/W</b>	oil-in-water
<b>OR</b>	Ostwald ripening
<b>PDI</b>	polydispersity index
<b>PDL</b>	poly(decylactone)

<b>PEG</b>	polyethylene glycol
<b>PLA</b>	polylactic acid
<b>PLGA</b>	polyglycolic acid
<b>ROP</b>	ring-opening polymerization
<b>TBD</b>	1,5,7-triazabicyclo [4.4.0]dec-5-ene
<b>UV-Vis</b>	ultraviolet-visible spectroscopy
<b>vdW</b>	van der Waals
<b>W/O</b>	water-in-oil

## 1 Introduction

### 1.1 Poorly soluble drugs

Oral route is the most common and convenient route of drug delivery, thanks to its ease of administration, high patient compliance and cost effectiveness (Shreya et al., 2019). Poor aqueous solubility in active pharmaceutical ingredients (APIs) is a restriction and challenge in drug development processes in pharmaceutical companies. Poor solubility is directly related to its bioavailability by decreasing the therapeutic effectiveness (Sareen et al., 2012; Murtaza et al., 2014). A poorly soluble drug is considered to have less than 0.1 mg/ml aqueous solubility, and the poor solubility can either be due to hydrophobicity or lipophilicity. Reports have suggested that 40% of drugs in clinical use are hydrophobic, and that 90% of new drug candidates in the pipeline fall into the Biopharmaceutics Classification System's Class II (high permeability, low solubility) or Class IV (low permeability, low solubility) categories (Custodio et al., 2008; Zhang et al., 2018). Aqueous solubility is a desirable property in a drug molecule to ensure delivery and interaction with the target. Successful drug discovery balances between hydrophobicity-driven potency and hydrophilicity-driven pharmacokinetic and pharmacodynamic action.

Hydrophobic molecules are considered as 'brick dust' molecules with strong intermolecular bonds within the crystal structure weakening the solubility. Lipophilic compounds, also called 'grease ball' compounds, are different in nature and do not follow the principle like dissolves like (Bergström et al., 2007). Fortunately, there are already strategies available for enhanced aqueous solubility by physical, chemical or other modification techniques, such as the use of surfactants, deep eutectic solvents and particle size reduction and nanotechnology (Kapourani et al., 2021; Chaudhary et al., 2012).

The  $\log P$  value is a simple parameter to predict the solubility of a substance rapidly. The  $\log P$  value is the logarithm of the n-octanol/water partition coefficient ( $P$ ) that can be determined empirically by phase-partitioning methods and provides a guideline for solubility characteristics in aqueous and organic solvents.  $\log P$  is a constant for any given compound describing the partition of non-ionizable or unionized forms of molecules between octanol and buffer (Hill & Young, 2010). 'Brick dust' molecules are considered to have a  $\log P$  value less than 2, and 'grease ball' molecules higher than 4 (Bibi et al., 2017).

## 1.2 Nanoemulsions as dosage forms

In the pharmaceutical industry, emulsion-based delivery systems are being used by encapsulating hydrophobic components into the core (Porter et al., 2007). Emulsion, in general, is a heterogeneous system of two immiscible liquids, either oil-in-water (O/W) (Figure 1) or water-in-oil (W/O). In addition to simple emulsions, there are also multiphase or double emulsions, meaning W/O/W or O/W/O. In double emulsions, normally two different surfactants (hydrophobic and hydrophilic) are utilized to satisfy the final result. Double emulsions are aimed especially for slow and sustained release (Binks, 2002). Emulsions are dispersions of oil and water stabilized by an interfacial film, and they can be manufactured with little energy input, such as heat or mixing (Tadros et al., 2013). The liquids are stabilized by an emulsifier or surfactant, which play a crucial role in fabrication of an emulsion. For instance, oil-in-water (O/W) emulsions, can be prepared by solubilizing the hydrophobic component inside the oil phase and homogenizing the phase with an aqueous phase containing water-soluble emulsifier.

The size of the droplets in the emulsion depends on the composition of the system, the homogenization method used and the feed rate. Conventional emulsions and nanoemulsions can be distinguished from each other based on the droplet shape and size: the mean droplet radius is typically <200 nm for nanoemulsions, and >200 nm for conventional emulsions (Jaiswal et al., 2014). To be stated, the droplet size varies significantly depending on the reference. The smaller droplet size in nanoemulsions means that the physicochemical and biological properties differ from the conventional emulsions.

Nanoemulsions have shown good potential in medical applications as a dosage form due to several advantages, such as delivery of drugs, masking of the disagreeable taste, protection of drug and non-toxicity (Jaiswal et al., 2015). To date, nanoemulsions have been used in the delivery of anti-cancer agents and vaccines (Najahi-Missaoui et al., 2020). Nanoemulsions can be rendered into several dosage forms, such as liquids, creams, sprays, gels, foams and aerosols and can, thereby, be administered by various routes, such as oral, topical, intranasal, pulmonary, intravenous, ocular and transdermal routes (Sharma et al., 2010; Singh et al., 2017). In lab scale, nanoemulsions are prepared simply by adding ingredients in proper order together with mechanical energy through agitation, sonication or high-speed stirrer mixer.



Because of their small droplet sizes, nanoemulsions have been shown to be more resistant to particle aggregation and gravitational separation (Solans et al., 2005; Sonneville-Aubrun et al., 2004). A key limitation is that they are thermodynamically unstable if the size exceeds 500 nm, meaning that the range of 20 to 200 nm is the most stable (Najahi-Missaoui et al., 2020; Kumar & Mandal, 2018). The small droplet size gives a clear or hazy appearance, which differs from the milky white color of the emulsion. Despite the droplet size being the same as in microemulsions, the structural aspects and long-term thermodynamic stability differ significantly from the microemulsions. A major criterion in manufacturing nanoemulsions is to achieve desired droplet size with monomodal distribution to ensure uniformity of properties and provide a good starting point for further fabrication (Singh et al., 2017). Nanoemulsions have a long shelf life and due to the nanosized droplets, the interfacial areas are enormous and thereby allow sustained and targeted drug delivery (Shafiq et al., 2007).

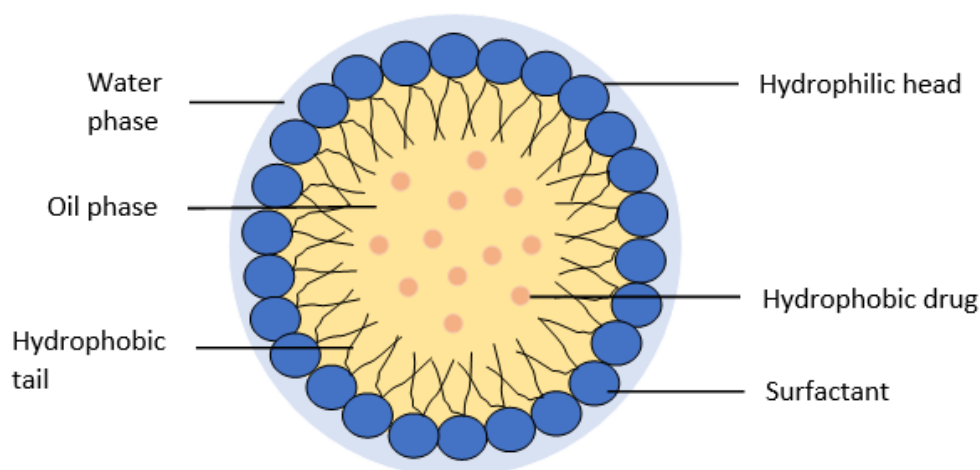


Figure 1. Structure of a O/W nanoemulsion.

### 1.2.1 Fabrication of nanoemulsions

Fabrication of nanoemulsions of a hydrophobic drug is a widely utilized approach to overcome the problem of poor aqueous solubility in drugs. Aqueous solubility of an active pharmaceutical ingredient (API) has a direct impact on the formulation strategies and bioavailability, which has to be taken into consideration. Nanoemulsions can be prepared by two methods: low-energy emulsification, such as phase inversion temperature and spontaneous emulsification, or high-energy emulsification, including high-energy stirring, microfluidization and membrane

emulsification (Jaiswal et al., 2015). Despite several advantages, there are still a few limitations associated with nanoemulsion, such as stability problems and cumbersome fabrication processes. However, nanoemulsion fabrication using an oily polymer instead of a conventional oil has been reported to overcome the problems associated with conventional methodologies (Wik et al., 2019). To be able to design a rational drug delivery system, the compatibility between drugs and polymer must be known.

### **1.2.2 Use of surfactants as stabilizers**

Stabilization surfactants are amphiphilic molecules having a tendency to accumulate in the oil-water interface. They reduce the oil-water interfacial tension minimizing the energy required for emulsion formation. The adsorption of the hydrophobic particles in the oil-water interface is a slow process and is enhanced by mixing. The adsorbed surfactant molecules act as electrostatic or steric barriers against coalescence at the interface resulting in increased stability of the emulsion (Aronson et al., 1978).

In general, there are two ways to stabilize an emulsion. The first way is electrostatic separation based on charge separation of electrical double layers. The most effective method to stabilize an emulsion is to use surface active polymers, polymeric surfactants, which not only adsorb strongly on the droplet surface but can also be applied in the presence of high electrolyte concentrations in high temperatures. The polymeric surfactant molecule can be designed to have an “anchor” and “stabilizing” chain giving a layer thickness of several nanometers (Katepalli, 2014; Tadros et al., 2004).

Another important application of surfactants is solubilization, which means that the solubility of a poorly water-soluble substance is increased (Lau, 2001). By adding a surfactant, a chemical that is ordinarily insoluble or marginally soluble in water is transformed into a thermodynamically unstable, isotropic solution by precipitation of the polymer (Tadros, 2003). Still, the selection of different surfactants in the preparation of emulsions is largely made on an empirical basis. One scale for selecting surfactants is the hydrophilic-lipophilic balance (HLB) developed by Griffin (Tadros et al., 2013). The HLB scale is based on the relative percentage of hydrophilic to hydrophobic groups in the surfactant molecule. In an O/W emulsion droplet, the hydrophobic chain resides in the oil phase and in a W/O emulsion, the hydrophilic groups

reside in the water droplet. Table I below presents a guide to the application of HLB. The HLB number depends on the nature of the oil (Tadros et al., 2013). The solubilization is mainly dependent on the surfactant concentration and type, meaning that to a certain point, the solubilization rate is increasing with increasing surfactant concentration. Also, the viscosity of the oil plays an important role in the breakup of droplets; the higher the viscosity, the longer it takes to deform a drop (Tadros et al., 2013).

Table I. HLB range gives a guide to the selection of surfactants for different applications. As an illustration, required HLB numbers for emulsification of different oils can be seen on the right (Tadros et al. 2013)

<b>HLB range</b>	<b>Application</b>	<b>Oil</b>	<b>W/O emulsion</b>	<b>O/W emulsion</b>
<b>3-6</b>	W/O emulsifier	<b>Paraffin Oil</b>	4	10
<b>7-9</b>	Wetting agent	<b>Beeswax</b>	5	9
<b>8-18</b>	O/W emulsifier	<b>Lanolin, anhydrous</b>	8	12
<b>13-15</b>	Detergent	<b>Cyclohexane</b>	-	15
<b>15-18</b>	Solubilizer	<b>Toluene</b>	-	15

### **1.2.3 Advantages of nanoemulsions**

Nanoemulsions have the potential to overcome many disadvantages in drug formulation. Therapeutic approaches of nanoparticles in general are, for instance, formulation of hydrophobic drugs/enhancement of solubility, targeting, controlled drug release, decreased side effects, increased local drug concentrations and biosensors (Figure 2). However, traditional approaches highly rely on the physicochemical properties, such as solubility and wettability. It has already been demonstrated that liposome, micellar, protein and polymeric nanoparticle formulations accomplish improved drug solubility, decreased early degradation of unstable drugs and improved circulation time, meaning that their pharmacokinetics and

pharmacodynamics are improved. As for nanoemulsions, together with optimum nanodroplet size and suitable components, the droplets can act as a reservoir of drugs, which means that nanoemulsions can be a multifunctional platform to treat diverse diseases, and increase the bioavailability of hydrophobic drugs (Krol, 2020; Nishitani Yukuyama et al., 2017).

Especially, when administered orally, the minimalistic size of the droplets increases the drug dissolution and bioavailability. The drug release from a nanoemulsion involves partitioning from oil into surfactant layer and finally into aqueous phase. It has also been reported that some nanoemulsions undergo direct lymphatic absorption, thereby avoiding first-pass metabolism and boosting bioavailability and thus, reducing the needed dose. To avoid nausea and associated non-compliance, nanoemulsions can be used to effectively screen bitter or metallic after taste of drugs (Singh et al., 2017).

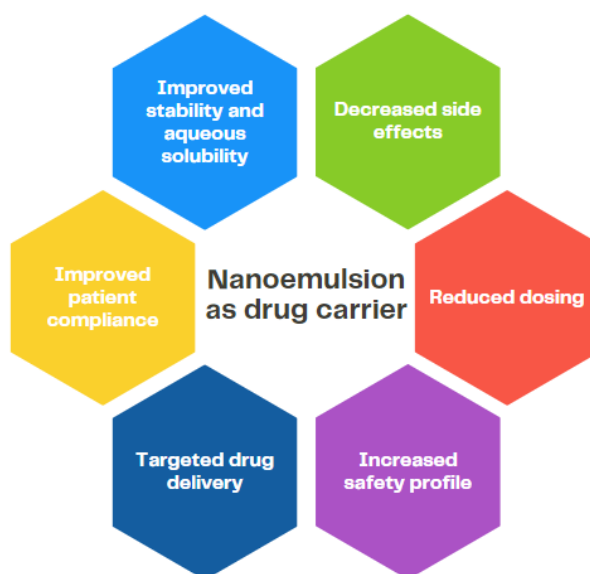


Figure 2. Principal advantages of nanoemulsions as drug carriers.

#### 1.2.4 Challenges with nanoemulsions

Nanoemulsions can be categorized into low-energy, high-energy and a combination of low- and high-energy nanoemulsions. Even though the nanoemulsion preparation methods are easy to apply, on a larger industrial scale they are not approved. One limiting major aspect of formulation components is non-toxicity (generally recognized as safe = GRAS excipients), especially if the product is intended for human use. In addition to formulation aspects, local

damage and toxicity have been reported, for example, with intranasal nanoemulsions. It is also established that the permeation enhancers, such as surfactants, can cause reversible or irreversible damage to the epithelium (Chatterjee et al., 2019).

When selecting suitable drugs for nanoemulsions, the physical properties, such as melting point, should be considered and, according to reports, nanoemulsions have a limited capacity to solubilize substances with a high melting point. Also, the temperature and pH of the nanoemulsion have an influence on the stability (Chime et al., 2014).

Nanoemulsions prepared by low-energy methods require large amounts of surfactants for stabilization of droplets. The major usage of surfactant can cause biomembrane fluidization, thus excluding their internal use. Price effectiveness of nanoemulsion manufacturing is profitable to consider in advance, as expensive instruments are often involved (Singh et al., 2017).

#### **1.2.4.1 Ostwald ripening and coalescence**

Ostwald ripening (OR) is the main mechanism of nanoemulsion breakdown. Emulsions are usually polydisperse and the smaller droplets tend to have higher solubility compared to the larger ones. Ostwald ripening is a phenomenon, which leads to phase separation and coarsening of emulsion, resulting in an increased droplet size. The mechanism behind is that the smaller droplets disappear, and the molecules diffuse to the bulk and attach on the larger droplets, resulting in larger values in droplet size distribution. Theoretically, an oil phase with very low aqueous solubility can prevent OR, but this is not always feasible.

In addition to OR, coalescence and other mechanisms also create instability and accelerated destabilization, that are presented in Figure 3. Coalescence is a result of kinetic phenomena, such as creaming, sedimentation or thermodynamic fluctuations, which lead to segregation or attachment of dispersed phase droplets. It is a process of thinning and disruption of the liquid film between the droplets, meaning that two or more droplets merge into larger ones. Coalescence is an event causing irreversible aggregation. In comparison to coalescence, sedimentation and creaming are reversible events, which can be counteracted through re-dispersion by shaking (Singh, 2017; Tadros et al., 2013).

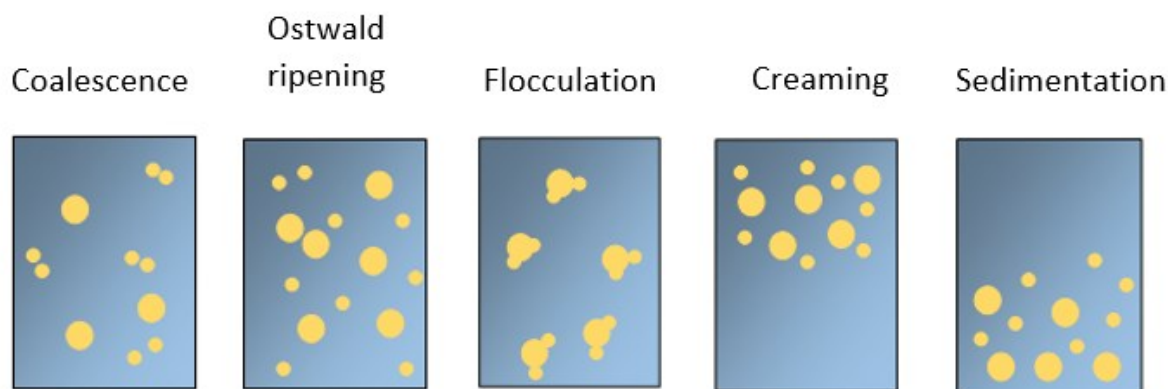


Figure 3. Destabilizing mechanisms of emulsions, that may lead to phase separation (adapted from Tayeb & Sainsbury, 2018).

### 1.3 Computational pharmaceuticals - Molecular dynamics simulations

Molecular dynamics simulations (MDS) are increasingly used in drug formulation design. Computational power has matured from a simple tool for single solute investigations into something, that allows many compounds to be rapidly screened for their compatibility with a certain solvent to help improving solubility, stability and other properties in drug formulations (Salo-Ahen et al., 2020). Nowadays, more and more complex systems are studied by utilizing MDS. Molecular dynamics (MD) provide a glimpse into the essential physics of a molecular system, including properties, such as dynamic behavior, stability, diffusion and vibration of the molecules. One major advantage is the possibility to study the inter- and intramolecular forces (van der Waals', electrostatic forces and strong bonded forces), that can be modeled by the so-called force field method (Hossain et al., 2019).

Experimental formulation and development are time-consuming and expensive. Computational pharmaceuticals provide versatile information to pharmaceutical scientists to facilitate this process (Ouyang & Smith, 2015). MD simulations convert experimental data into numerical answers and provide crucial information by knowing fundamental drug-polymer interactions, such as nanoparticle size, drug release profile, drug-loading capacity and stability (Salo-Ahen et al., 2020; Stipa et al., 2019). Figure 4 presents the principal steps in MDS.

Cost-efficiency and speed are the major advantages of MDS. In particular, MD simulations decrease the number of expensive and tedious experimental assays and thereby decrease the

costs. With rapidly growing theory, hardware- and software algorithms, computer simulations can model complex systems, that may even be impractical to measure by experiments. Overall, MDS have born fruit in advanced mechanisms for drug delivery, including solubility and compatibility studies, especially in nanomedicine (Rog & Bunker, 2020).

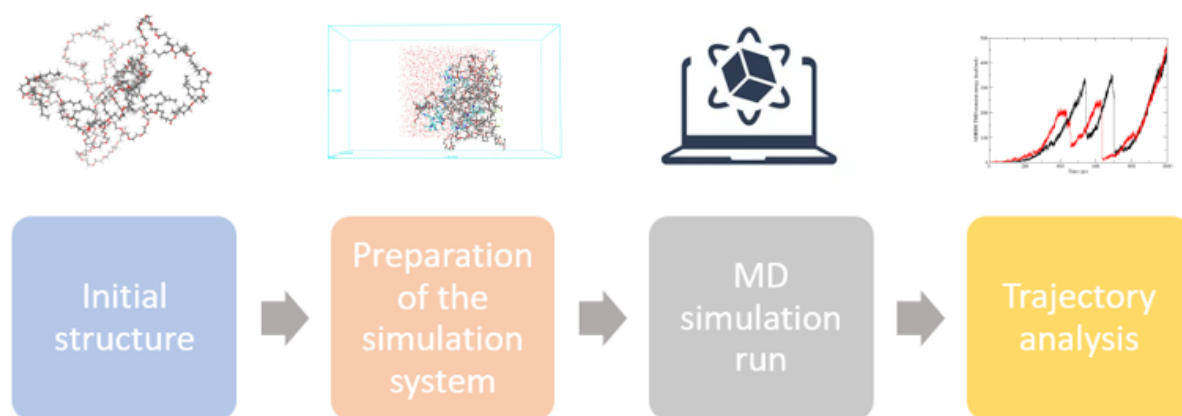


Figure 4. A simple flowchart of the principal steps in molecular dynamics simulations (adapted from Profacgen n.d.).

### 1.3.1 Application of MDS when predicting miscibility

In a polymeric system, compatibility between drug and polymer governs the loading capability based on the concept ‘like-dissolve-like’. The easiest and most common approach to investigate the interactions between a drug and a polymer is to select drugs with different lipophilicity, meaning drugs with different  $\log P$  values. In a study by Stipa et al. (2019), polylactic acid (PLA) and polyglycolic acid (PLGA) carriers with three APIs having different  $\log P$  values were simulated, resulting in clear differences in the behavior. The results were in line with the different lipophilicities of the molecules. Isoniazid ( $\log P = -1.1$ ) showed hydrophilic character by diffusing out from the carrier to interact with water and ions. Paracetamol ( $\log P = 0.3$ ) showed high tendency to interact with polar groups of polymers, especially at the surfaces. Finally, prednisolone ( $\log P = 1.6$ ) showed tendency to retain itself in the core of the polymer, favoring prednisolone-prednisolone interactions (Stipa et al., 2021). MD simulations have also been used to achieve better design and administration of controlled release systems and to predict the transport properties of the drug and the biologic fluid (Subashini et al., 2011).

### 1.3.2 Hildebrand & Hansen solubility parameter

Compatibility between a drug and a polymer can also be determined, for instance, via Hildebrand and Hansen solubility parameters utilizing the intramolecular bond strength. The Hildebrand solubility parameter is one of the oldest measures of solvent polarity and utilizes a single parameter,  $\delta$ , defined as the square root of the cohesive energy density (CED) (Weerachanchai et al., 2014). CED is a measure of the intramolecular bond strength determining whether a substance is a good solvent or nonsolvent. CED of a liquid is a numerical value indicating the energy of vaporization and directly reflecting the degree of van der Waals forces, that hold the molecules of the liquid together. The stronger the intramolecular bond strength is, the higher the heat of vaporization-value  $\Delta H_v$  is. In other words, the correlation also translates into a similar solubility behavior, because the same intermolecular attractive forces must be separated to vaporize a liquid as to dissolve it. Since the solubility of two materials is possible only when the intermolecular forces are similar, it can also be expected that only materials with similar CED values would be miscible. Thereby, CED can be utilized to determine whether a substance is a good solvent or nonsolvent (Burke, 1984). The square root of the CED or Hildebrand solubility parameter can be calculated as follows:

$$\delta = \sqrt{CED} = \left[ \frac{\Delta H_v - RT}{V_m} \right]^{1/2}$$

where  $R$  is the gas constant,  $T$  is temperature in Kelvin, and  $V_m$  is the molar volume. Solvents with a  $\delta$  value ranging between  $-2$  and  $+2$  MPa<sup>1/2</sup> from the solute's  $\delta$  value are considered good solvents and the values outside that range are deemed nonsolvents for the particular solute (Figure 5) (Venkatram et al., 2019). In comparison to the theory of  $\pm 2$  MPa<sup>1/2</sup> distance in the solubility parameters of two substances, Forster et al. (2001) reported that substances with a solubility parameter difference of  $<7.0$  MPa<sup>1/2</sup> show significant miscibility and a difference  $>10$  MPa<sup>1/2</sup> indicates immiscibility. In sum, the Hildebrand solubility parameter approach gives simple predictions of phase equilibrium based on a single parameter and can also be used when predicting swelling of polymers by solvents. However, one limiting aspect is that the parameter varies with temperature (Hancock et al., 1997).



The Hansen model, in turn, utilizes three parameters,  $\delta D$ ,  $\delta P$ , and  $\delta H$ , to quantify solvent-solute compatibility. These parameters represent the dispersion, polar and hydrogen-bonding components. A single parameter  $\delta$  can be calculated as the square root of the following equation:

$$\delta^2 = \delta D^2 + \delta P^2 + \delta H^2$$

If visualized as a three-dimensional plot, the axes are  $2\delta D$ ,  $\delta P$  and  $\delta H$ , and the solutes and solvents are represented by points. The solvents within a sphere of radius  $R = 8 \text{ MPa}^{1/2}$  centered at a point corresponding to a solute are considered as good solvents, and the solvents that are outside the sphere are considered nonsolvents (Venkatram et al., 2019). Compared to the Hildebrand solubility parameter, the Hansen solubility parameter considers the interactions between molecules and is thereby more practical in a polymerization system (Abbott & Hansen, 2008). Nevertheless, in this thesis, only the Hildebrand solubility parameter will be considered in the results.

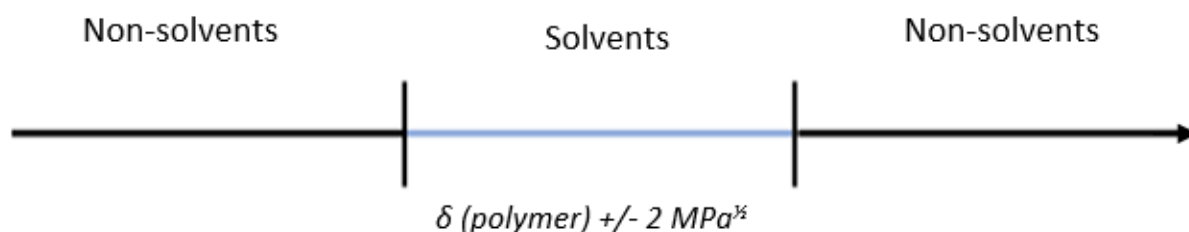


Figure 5. Solubility model of the Hildebrand solubility parameter. The solvent is considered to be good, if the value  $\delta$  does not differ with more or less than  $2 \text{ MPa}^{1/2}$  of the solute's (here, polymer) value (adapted from Venkatram et al., 2019).

## **2 Aim**

The objective of this study was to develop a polymeric O/W nanoemulsion formulation with high drug solubilization capacity and stability. The compatibility between hydrophobic drugs and polymer is a key factor affecting the drug solubilization in polymers and has a direct impact on the drug encapsulation in that particular polymeric system. Therefore, in this study, the miscibility of poly(decylactone) (PDL) polymer and different hydrophobic drugs was predicted by using the Hildebrand solubility parameters calculated from MD simulations. The theoretical values were confirmed with experiments by fabricating the nanoemulsion using earlier reported procedures. The surfactant was synthesized by using polyethylene glycol (PEG) as the hydrophilic moiety and PDL as the hydrophobic moiety to generate a diblock amphiphilic copolymer. The in-house synthesized surfactant was utilized to investigate its capability to stabilize the nanoemulsion. Finally, the results were compared with a commercially available surfactant Kolliphor P 188 to ascertain the effectiveness of the PDL-based polymeric surfactant.

### **3 Materials and methods**

#### **3.1 Materials**

Indomethacin and furosemide were purchased from Fagron Nordics A/S, Copenhagen, Denmark. Dexamethasone (>99%) was purchased from TCI, Tokyo, Japan. Methotrexate hydrate ( $\geq 98\%$ ) was obtained from Sigma-Aldrich, United Kingdom. Sorafenib free base, sunitinib free base and celecoxib (>99%) were purchased from LC Laboratories, Woburn, USA. Itraconazole (PARAM012, unknown (gifted)). Methanol for HPLC ( $\geq 99.9\%$ ) and acetone for HPLC ( $\geq 99.8\%$ ) were procured from Sigma-Aldrich, France and Israel. Kolliphor P 188 was purchased from BASF SE, Ludwigshafen, Germany. Deionized water was house-made (Milli-Q Synthesis, Millipore, Molsheim, France). The 0.2  $\mu\text{m}$  polyethersulfone membrane filters and 0.45  $\mu\text{m}$  polypropylene membrane filters were purchased from VWR (Puerto Rico and China).

## 3.2 Methods

### 3.2.1 Selection of APIs

The aim was to find eight hydrophobic APIs with suitable  $\log P$  value and low aqueous solubility ( $<0.1$  mg/ml) (Chaudhary et al., 2012). Also, the Hildebrand solubility parameters after the MDS were considered, because we aimed to select APIs with various solubility values to achieve clearer results. Therefore, the first step was to find multiple suitable drug molecules from PubChem database and Schrödinger's Maestro molecular modeling suite. Finally, the eight active pharmaceutical ingredients selected to this study were celecoxib, dexamethasone furosemide, indomethacin, itraconazole, methotrexate, sorafenib and sunitinib. The 2D structures of each API are presented in Figure 6.

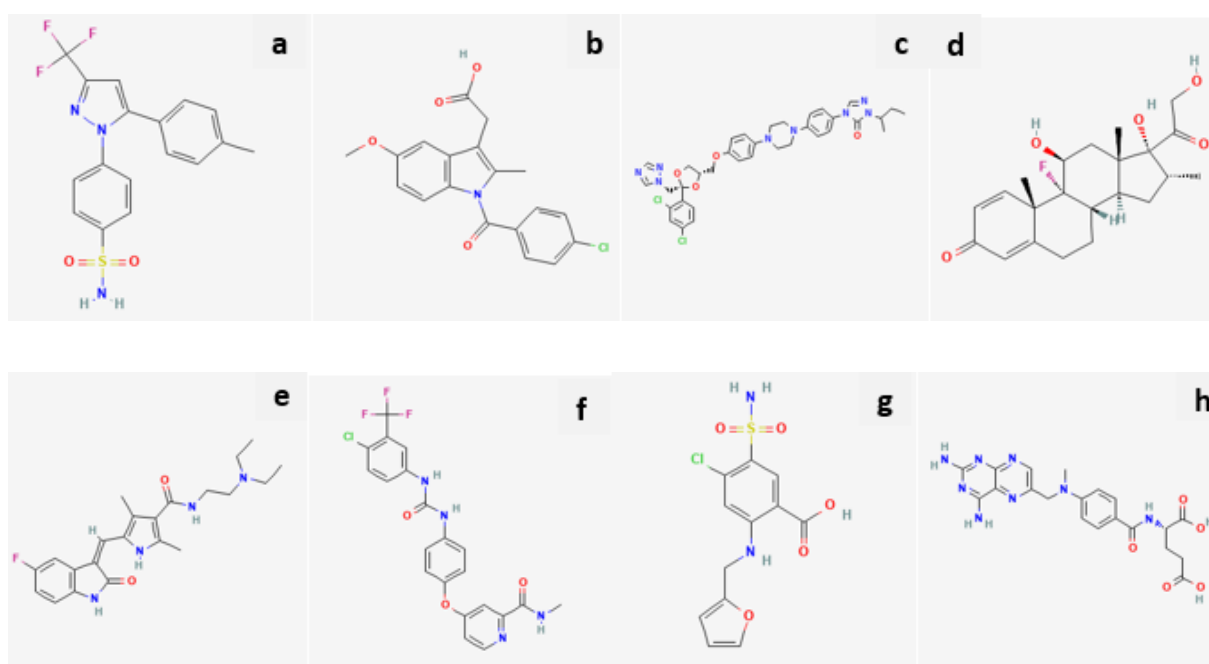


Figure 6. The 2D structures of a) celecoxib, b) indomethacin, c) itraconazole, d) dexamethasone, e) sunitinib, f) sorafenib, g) furosemide and h) methotrexate. Source: PubChem (Kim et al., 2021).

### **3.2.2 Computational assessment**

The MD simulations were performed using Desmond (Bowers et al., 2006) via Schrödinger's Maestro Materials Science suite release 2020-4 (Schrödinger, LLC, New York, NY, 2020) to determine the Hildebrand solubility parameters for different hydrophobic drugs, PDL polymer and mPEG-b-PDL.

#### **3.2.2.1 Polymer modeling**

The polymer structure consisting of a starting group (initiator), monomer unit and ending group (terminator) was sketched using the Polymer Builder tool of the Maestro Materials Science suite. To build up the homopolymer PDL, a length of 102 monomers was decided, whereafter monomers of lactone moieties were added. Totally, 10 polymer chains were added to the amorphous system. The backbone dihedral angle was set to random, and the clashes between C-C and C-H atoms were avoided by specifying the van der Waals scale factor to 0.50 and seeding was set to random.

When preparing the mPEG-b-PDL co-polymer, homopolymers of PDL and PEG5000 were built separately as described above for plain PDL. The length of the PDL and PEG was 19 and 80 monomers, respectively. Finally, the copolymerization was achieved by addition of blocks of PDL and PEG in turn by using Co-polymer Builder tool of the Maestro Materials Science suite.

#### **3.2.2.2 Simulation system preparation**

When preparing the simulation systems for the polymers, the plain PDL polymer and the mPEG-b-PDL co-polymer were loaded to the workspace individually. The maximum number of polymer chains was 10 for the PDL, and 15 for mPEG-b-PDL. The initial density was  $0.5 \text{ g cm}^{-3}$  and periodic boundary conditions (PBC) with an orthorhombic unit cell were used for all simulations. The initial disordered system was set to a tangled chain using the OPLS3e force field (Roos et al., 2019).

For the APIs, the preparation for the simulation differed a little from the polymer path. The 2D structures of the drugs were imported from the PubChem database (file type .sdf) into Maestro and processed by a tool called LigPrep. The structures were desalted, neutralized and energy-minimized in the OPLS3e force field. Specified chiralities were retained. To prepare an amorphous system of the individual drug molecules, the Disordered System Builder was used to build 300 copies of the original structure. An orthorhombic simulation box with PBC was used. Otherwise, the same steps from MD Multistage Workflow onwards were performed for the selected drugs as for the polymer and surfactant.

### **3.2.2.3 Molecular dynamics simulations**

When the polymer and drug simulation systems had been prepared, the MD Multistage Workflow tool of Maestro, that employs the Desmond MD algorithm, was used to carry out the MD simulations. A three-stage material relaxation protocol was used, and the MD simulations were carried out in the NTP ensemble for 2 ns using a time step of 2 fs. The trajectory snapshots were recorded every 40.0 ps. The distance from all sides of the simulation box to the solute was set to 10 Å. To speed up the simulation, the files were transferred with an open-source software named FileZilla (<https://filezilla-project.org>) from the local host (desktop computer) to the remote host (supercomputer Puhti at CSC – IT Centre for Science; [www.csc.fi](http://www.csc.fi)) to execute the simulation.

Finally, Maestro Materials Science (MS) MD Trajectory Analysis panel was used to obtain the simulation report of the various bulk properties of the drug and polymer systems. The properties included volume, density, cohesive energy, solubility parameter and heat of vaporization. Further analysis of the raw data obtained from the simulations was processed with Microsoft Excel.

In Schrödinger Material Science suite, the **cohesive energy** ( $E_{coh}$ ) is defined as the energy of the cell ( $E_{cell}$ ) divided by the number of molecules ( $N$ ) in the cell, minus the energy of a single molecule in the gas phase ( $E_{mol}$ ):

$$E_{coh} = (E_{cell} / N) - E_{mol}$$

The **Hildebrand solubility parameter**  $\delta$  for a pure liquid is defined as:

$$\delta = [(\Delta H_v - RT)/V_m]^{1/2}$$

where  $\Delta H_v$  is the heat of vaporization and  $V_m$  is the molar volume. In addition to the solubility parameter, the van der Waals (vdW) and electrostatic contributions to (the square of) this quantity can be selected and plotted in Maestro Materials Science suite.

The **heat of vaporization** is calculated from the energy of the periodic unit cell minus the sum of the  $N$  individual molecules,  $E_i$ , averaged over the MD trajectory, as:

$$\Delta H_v = \langle E_{cell} - \sum_i E_i \rangle + RT.$$

The **Hildebrand Distance** ( $D_H$ ) utilizes a single parameter  $\delta$ , defined as the square root of the cohesive energy density ( $CED$ )

$$D_H = \delta_1 - \delta_2$$

where  $\delta_1$  and  $\delta_2$  are the solubility parameter values of substance 1 (polymer) and 2 (API). Shorter distance indicates miscibility while longer suggests immiscibility.

### 3.2.3 Synthesis of homopolymer PDL and block copolymer mPEG-b-PDL

Polymers PDL and mPEG-b-PDL (methoxy-poly(ethylene glycol)-b-poly(decylactone)) were synthesized according to the reported method. An organic catalyst was used through ring opening polymerization (ROP) of monomer decylactone in the absence of solvent utilizing propargyl alcohol and mPEG<sub>5k</sub> (gifted by Rosenholm et al. lab group) as initiators. The synthesis and characterization of homopolymer PDL was already reported in a previous publication from our laboratory, and the same method was used in this study (Wik et al., 2019).

For the synthesis of the block copolymer mPEG-b-PDL, methoxyPEG (20.0 g, 4.0 mmol) and  $\delta$ -decylactone (44.2 g, 260.0 mmol) was heated up to 50 °C under high vacuum and stirred for 20 minutes, to remove the moisture residues. Next, vacuum was removed, and nitrogen gas was added to the flask followed by addition of 1,5,7-triazabicyclo [4.4.0]dec-5-ene (TBD) (0.9 g, 6.5 mmol). The mixture was stirred for 7 hours at 50 °C under an inert atmosphere. The reaction mixture was cooled, and benzoic acid (2.5 g, 20.4 mmol) solution in acetone (5 ml) was added to quench the reaction, followed by precipitation of the polymer in cold methanol. Any residual solvent was removed in vacuum, and the dry material was again dissolved in a minimum quantity of acetone, followed by re-precipitated petroleum ether to remove homopolymer excess. Finally, the precipitated polymer was dried in vacuum to yield the desired copolymer, being a sticky and white solid. The target molecular weight was near to 8.0 kDa to match the molecular weight of Kolliphor P 188, where mPEG5k was used as initiator to generate diblock copolymer. Characterization from proton nuclear magnetic resonance (<sup>1</sup>H NMR) for mPEG-b-PDL was as follows:

mPEG-b-PDL: <sup>1</sup>H NMR (500 MHz, CDCl<sub>3</sub>)  $\delta$  (ppm) 4.88 (CH-O-CO, m,  $J = 5.7$  Hz, 19H), 4.26–4.17 (CH<sub>2</sub>-O-CO, t, 2H), 3.85 – 3.47 (O-CH<sub>2</sub>-CH<sub>2</sub>-O, m, 511H), 3.39 (O-CH<sub>3</sub>, s, 3H), 2.42 – 2.23 (O-CO-CH<sub>2</sub>, m, 39H), 1.81 – 1.41 (CH<sub>2</sub>-CH<sub>2</sub>-CH-CH<sub>2</sub>, m, 114H), 1.39–1.16 (CH<sub>2</sub>-CH<sub>2</sub>-CH<sub>2</sub>-CH<sub>3</sub>, m, 118H), 1.00 – 0.80 (CH<sub>2</sub>-CH<sub>3</sub>, t, 60H) (Pyrhönen et al., 2022).



### **3.2.4 Preparation of standard curves**

A stock solution of 1 mg/ml was prepared for all of the drugs. First, 5 mg of drug and 5 ml of methanol were mixed in a vial on a magnetic stirrer. From these stock solutions appropriate dilutions, depending on the drug in question, were prepared in the range of 2-100 µg/ml for all eight drugs. Dilutions were made both with water and methanol to obtain two different standard curves and later, the more favourable was selected. The absorbances were measured and the peaks were detected with ultraviolet-visible spectrophotometry (UV-Vis) (NanoDrop 2000c, Thermo Scientific, USA). Depending on the selected diluent, either water or methanol was used as blank. Due to light sensitivity, indomethacin, dexamethasone, furosemide, and methotrexate samples were protected from light for their whole shelf life.

### **3.2.5 Determination of aqueous solubility of pure drugs**

The determination of water solubility was performed by the shake flask method. The samples were prepared by weighing approximately 2 mg of drug and 2 ml of water into Eppendorf tubes to achieve saturated solution, and 3 samples of each API, were placed on a magnetic stirrer for 3 days followed by one day of equilibration. On day 4, the samples were centrifuged at 13,500 RPM for 10 min and filtered through a 0.2 µm polyethersulfone membrane filter to remove undissolved API. The water solubility was measured as such after centrifugation and filtration without dilution, except methotrexate and dexamethasone, which were diluted with water, containing 200 µl of solution and 800 µl of water to reach appropriate absorbance levels. The concentrations were then calculated by using pre-prepared standard calibration curves.

### **3.2.6 Preparation of nanoemulsion**

Preparation of nanoemulsion was performed by low-energy emulsification called nanoprecipitation, also known as spontaneous emulsification. PDL polymer was used as oil and mPEG-b-PDL as surfactant. To obtain a drug-loaded oil-in-water nanoemulsion, the drug (5 mg), PDL (25 mg) and mPEG5k-b-PDL3k surfactant (75 mg) were dissolved in acetone (1.5 ml) followed by vortex and sonication. This organic mixture was added dropwise into water (5 ml), that was stirring in an open vial for at least 3 h at room temperature to ensure the

complete removal of organic solvent (acetone). In this study, the mPEG-b-PDL was added into the organic mixture to ensure the solubility of the sticky solid. Compared to earlier studies, the surfactant has been added into the water phase. Finally, before characterization, the nanoemulsion was centrifuged (Microcentrifuge Scanspeed, Labogene, Lynge, Denmark) for 10 min at 13,500 RPM and filtered through a 0.45  $\mu\text{m}$  polypropylene membrane filter.

For comparison, a similar solution was prepared by using Kolliphor P 188 instead of in-house-made surfactant. Kolliphor P 188, also known as Pluronic F-68 or Poloxamer-188, is an FDA-approved, non-toxic, biodegradable and biocompatible emulsifier and solubilizer, which is used to improve the solubility among others (Loureiro & Pereira, 2020).

As mentioned above, the organic mixture was added into water, but in the experiments with Kolliphor P 188, water and surfactant were mixed before the organic mixture was added. At the very beginning, blank nanoemulsions were prepared using 50, 75, and 100 mg surfactant to examine and decide the minimum appropriate level creating a stable emulsion.

### **3.2.7 Characterization of nanoemulsion**

#### **3.2.7.1 Drug content**

The drug content and water solubility were determined by using ultraviolet-visible spectrophotometry (UV-Vis). The drug content samples of nanoemulsion were prepared by pipetting 10-100  $\mu\text{l}$  of the filtered emulsion into an Eppendorf tube to reach appropriate absorbance levels that were dependent on the API. The step was followed by addition of deionized water or methanol up to 100  $\mu\text{l}$  and vortex. The diluents are presented in Table III. Drug content measurements were performed at days 0, 30 and 60.

#### **3.2.7.2 Droplet size of nanoemulsion**

The droplet size and polydispersity index (PDI) of the emulsions were analyzed by dynamic light scattering (DLS) on a Zetasizer (Nano ZS version 7.12, Malvern Instruments, Worcestershire, UK). The light used in the instrument is sourced from Helium-Neon laser with

a wavelength of 633 nm. The samples were prepared by pipetting 10  $\mu\text{l}$  of emulsion and 990  $\mu\text{l}$  (50  $\mu\text{g}/\text{ml}$ ) of deionized water followed by vortex and sonication. The samples were then transferred into cuvettes and measured at 25  $^{\circ}\text{C}$ . Measurements were performed at days 0, 30 and 60.

### **3.2.7.3 Nanoemulsion stability study**

The stability of drug-loaded samples was evaluated by high-speed centrifugation for 30 min at 13,500 RPM at fresh. The samples were stored for long-term stability studies for two months at room temperature ( $20 \pm 2$   $^{\circ}\text{C}$ ). Samples were analyzed visually for separation. Changes in size and drug content were analyzed via DLS and UV-Vis spectroscopy every 30 days as described in 3.2.7.1 and 3.2.7.2.

## 4 Results

### 4.1 Computational assessment of polymer/API bulk properties

In the computational assessment, various bulk properties, such as Hildebrand solubility parameter ( $\delta$ ), density, heat of vaporization and cohesive energy were calculated for PDL, mPEG-b-PDL and the APIs. The values are presented in Table II. The Hildebrand distances ( $D_H$ ) were calculated as the difference between the solubility parameters of the polymer and APIs, and surfactant and API.

Table II. MD-predicted bulk properties for the studied polymers and APIs and the calculated Hildebrand distances ( $D_H$ ) for PDL-API and mPEG-b-PDL-API mixtures

Polymer/API	Density (g cm <sup>-3</sup> )	Heat of vaporization (kcal mol <sup>-1</sup> )	Cohesive energy (kcal mol <sup>-1</sup> )	Hildebrand solubility parameter ( $\delta$ ) (MPa <sup>1/2</sup> )	$D_H$ (MPa <sup>1/2</sup> )  PDL and API	$D_H$ (MPa <sup>1/2</sup> )  mPEG-b- PDL and API
PDL	0.95	787.11	786.52	13.39	-	-
mPEG-b-PDL	1.03	397.82	397.22	16.30	-	-
Celecoxib	1.8	10.82	10.23	14.22	0.83	2.08
Indomethacin	1.69	14.10	13.51	16.34	2.95	0.04
Itraconazole	1.64	30.74	30.14	17.13	3.74	0.83
Dexamethasone	1.15	36.20	35.60	20.92	7.53	4.62
Sunitinib	1.11	41.17	40.57	21.74	8.35	5.44
Sorafenib	1.37	46.66	46.07	23.8	10.41	7.50
Furosemide	1.45	38.46	37.87	26.31	12.92	10.01
Methotrexate	1.25	67.28	66.68	27.69	14.3	11.39

As mPEG-b-PDL is copolymerized with PEG, the hydrophilicity of the polymer rises, resulting in an increase in the solubility parameter, and an overall decrease in cohesive energy when compared to plain PDL. In general, a higher solubility parameter value suggests a greater solvent polarity (Weerachancai et al., 2014). In Figure 7, the solubility parameter values and  $D_H$  can be seen in a plot.

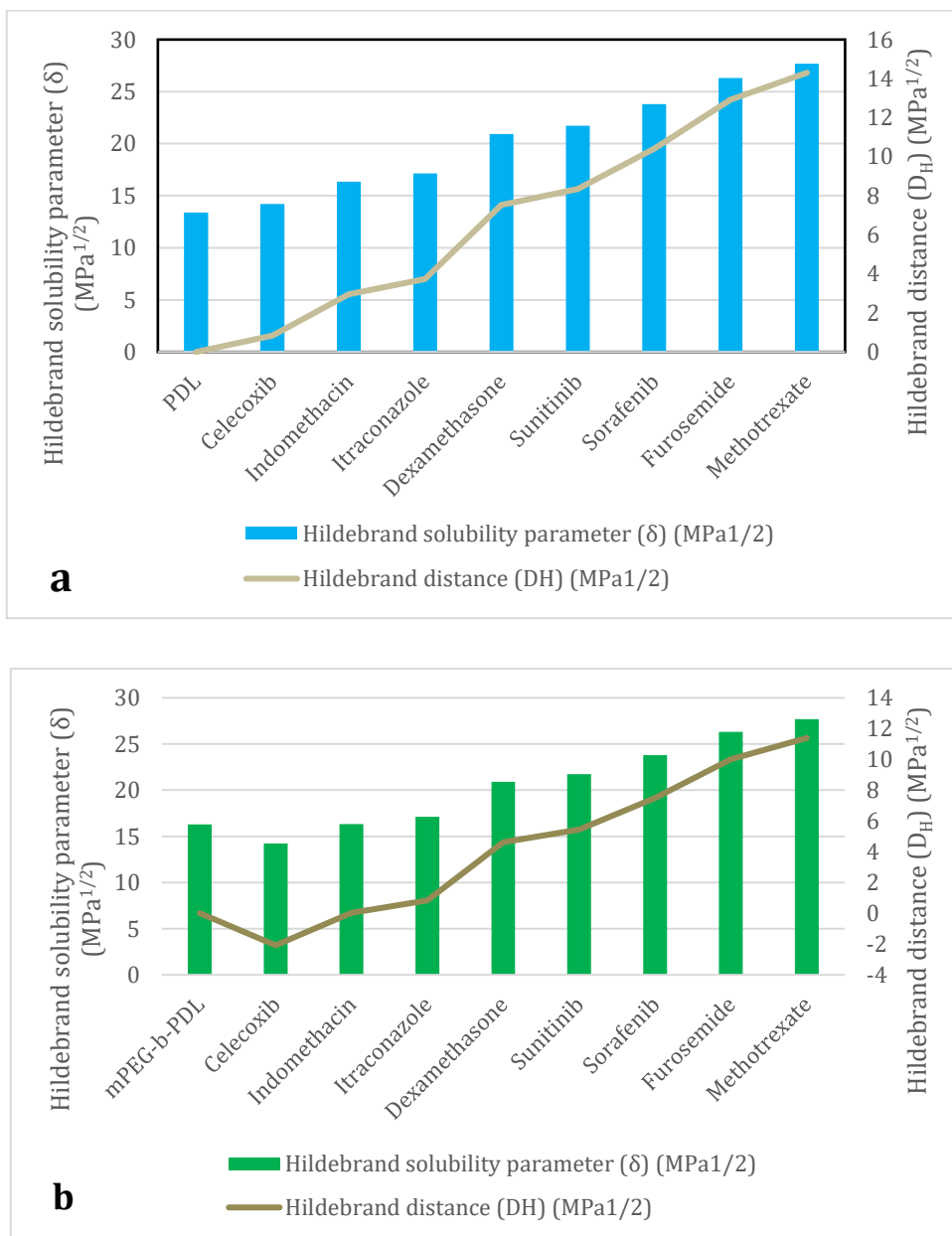


Figure 7. Comparison between Hildebrand solubility parameter ( $\delta$ ) and Hildebrand distance ( $D_H$ ) calculated between API-PDL and API-(mPEG-b-PDL). Bars represent the solubility parameter ( $\delta$ ) and lines the distance ( $D_H$ ).

Based on these findings, the order of API miscibility in PDL is: celecoxib > indomethacin > itraconazole > sunitinib > sorafenib > furosemide > methotrexate, and in mPEG-b-PDL the order is otherwise the same, except for celecoxib that was ranked between itraconazole and sunitinib. Celecoxib, indomethacin and itraconazole are assumed to be miscible in both PDL and mPEG-b-PDL. However, sunitinib was predicted to be miscible only in the mPEG-b-PDL. In these polymers, the rest of the APIs were likely to be non-miscible or partially miscible (sorafenib in the copolymer).

In Figure 8, it can be observed that copolymerization increases the overall flexibility of the polymer, thus reducing the persistence length and radius of gyration for mPEG-b-PDL compared to PDL. The persistence length of a polymer is a fundamental mechanical feature that can be used to distinguish between polymers that behave like a flexible or a stiff rod (Pyrhönen et al., 2022).

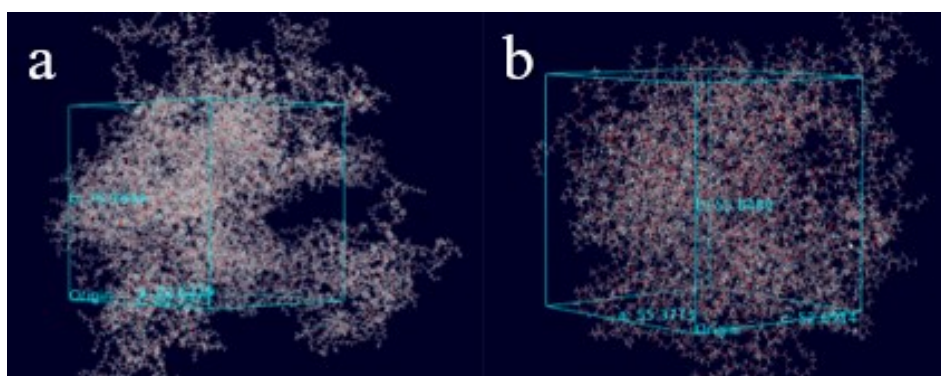


Figure 8. Snapshot of the simulation frame from the MDS a) PDL polymer (stiffer), and b) mPEG-b-PDL copolymer (more flexible) (Pyrhönen et al., 2019).

## 4.2 Synthesis and characterization of PDL homopolymer and block copolymer surfactant

The synthesis and characterization data of homopolymer PDL (Figure 9) was reported in a previous publication and the same polymer was used in this study (Wik et al., 2019). The average molecular weight determined by size exclusion chromatography for PDL polymer was 9.4 kDa with a polydispersity index (PDI) of 1.21. The block copolymer surfactant of poly(decylactone), i.e. mPEG-b-PDL, was synthesized using mPEG<sub>5k</sub> as initiator according to the following procedure (Figure 9). The synthesis and characterization of PDL polymer and surfactant were performed by Dr. Kuldeep Bansal.

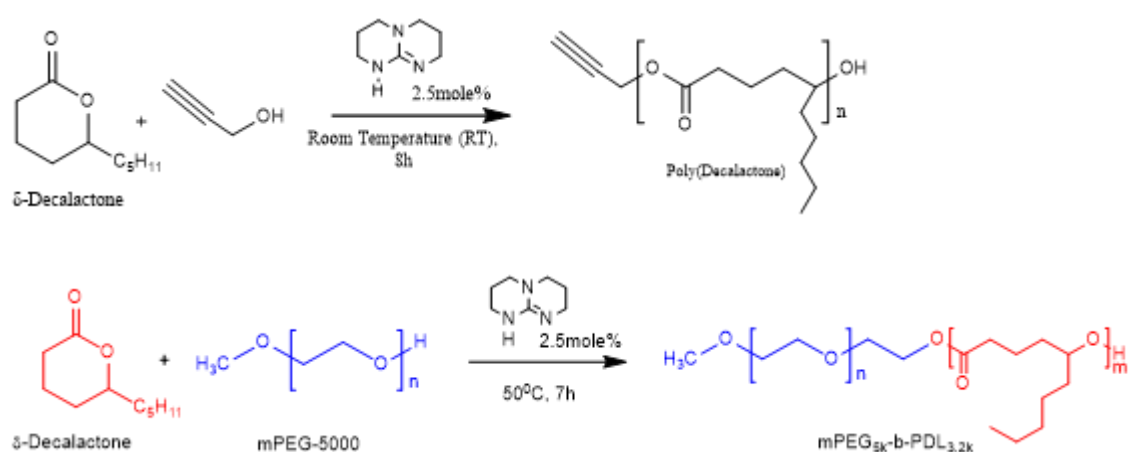


Figure 9. Synthesis figure of poly(decylactone) homopolymer (top) and copolymer mPEG-b-PDL (bottom) (Pyrhönen et al., 2022).

As demonstrated in the study by Wik et al. (2019), mPEG-b-PDL is an amphiphilic polymer that can self-assemble into micelles with low critical micelle concentration (CMC) values and can thereby act as a potential surfactant. The hydrophobic chain length of mPEG-b-PDL was low in this study to increase the aqueous solubility of the copolymer and to match it with the molecular weight of Kolliphor P 188, being 8350 Da. It can be stated that the synthesis and purification of mPEG-b-PDL were successful when all peaks in  $^1\text{H}$  NMR matched with the earlier reported values. As in  $^1\text{H}$  NMR, mPEG-b-PDL contained  $\sim 19$  repeating units of PDL considering the proton integrals at 4.8 ppm (Figure 10), corresponding to a molecular weight of 3.2 kDa. Thereby, 5 kDa of mPEG was used as initiator, because the molecular weight of mPEG-b-PDL by  $^1\text{H}$  NMR was calculated to be 8.2 kDa.

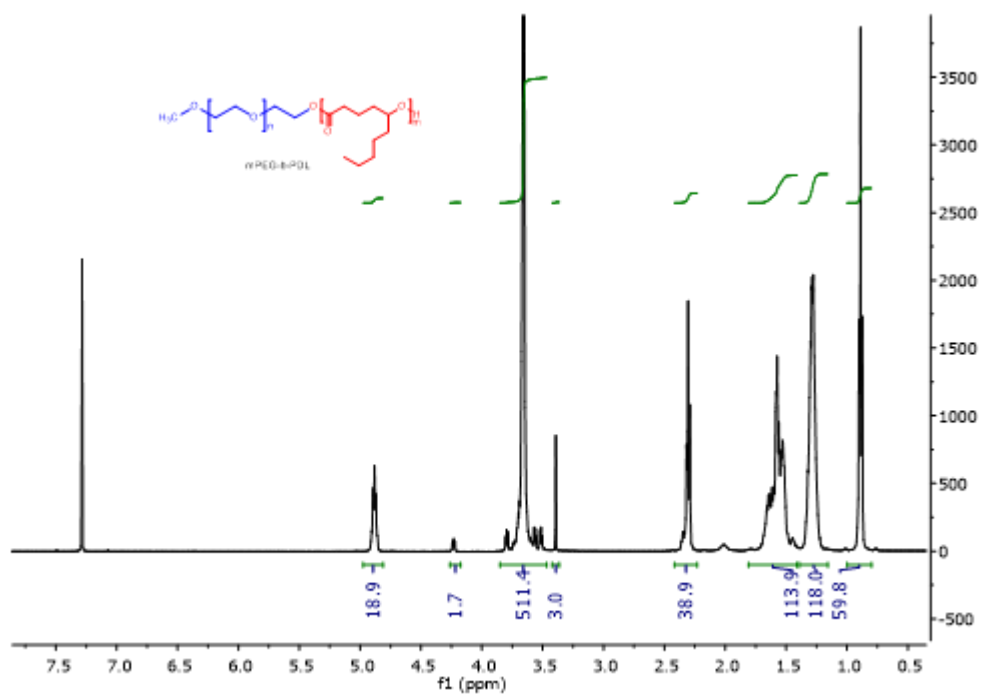


Figure 10.  $^1\text{H}$  NMR spectra of mPEG-b-PDL. The molecular weight of the copolymer was calculated by comparing the proton resonance of mPEG at 3.3 ppm and ring-opened PDL at 4.8 ppm (Pyrhönen et al., 2022).



### 4.3 Standard curves

Nanoemulsion samples were analyzed by UV-Vis after appropriate dilutions to determine the drug concentration. Using the calibration curves that had been created for this study, the amount of drug present in samples was calculated. The solvents for the measurements and the  $\lambda_{\max}$  are presented in Table III. Instead of water, methanol was selected as solvent for three APIs to obtain more reliable and stable spectra. The UV spectra recorded for the calibration curves for the APIs that were UV analyzed are shown in Figure 11. Finally, Figure 12 shows the calibration curves and equations used for determining the drug content and aqueous solubility of each API. Several absorbances that were deviating from the regression line were excluded to achieve higher  $R^2$  values. The  $R^2$  values exceeded 0.98 in all APIs indicating reliable correlation.

Table III. The solvents and  $\lambda_{\max}$  (nm) for each API

<b>Drug</b>	<b>Solvent</b>	<b><math>\lambda_{\max}</math> (nm)</b>
Celecoxib	Methanol	252
Indomethacin	Water	318
Itraconazole	Water	267
Dexamethasone	Water	241
Sunitinib	Water	423
Sorefenib	Methanol	265
Furosemide	Water	331
Methotrexate	Methanol	265

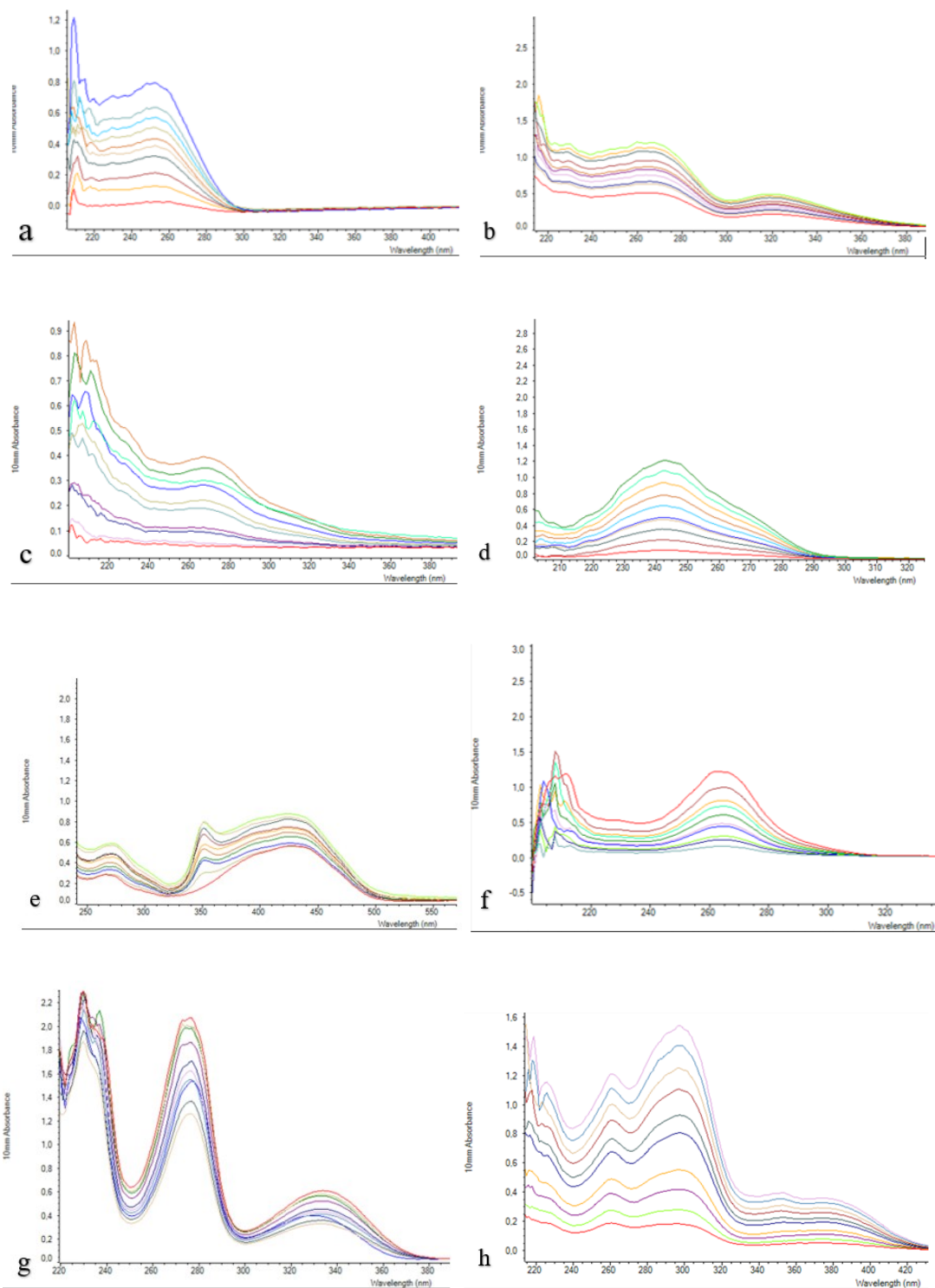


Figure 11. UV-Vis spectra of all APIs: celecoxib (a), indomethacin (b), itraconazole (c), dexamethasone (d), sunitinib (e), sorafenib (f), furosemide (g) and methotrexate (h).

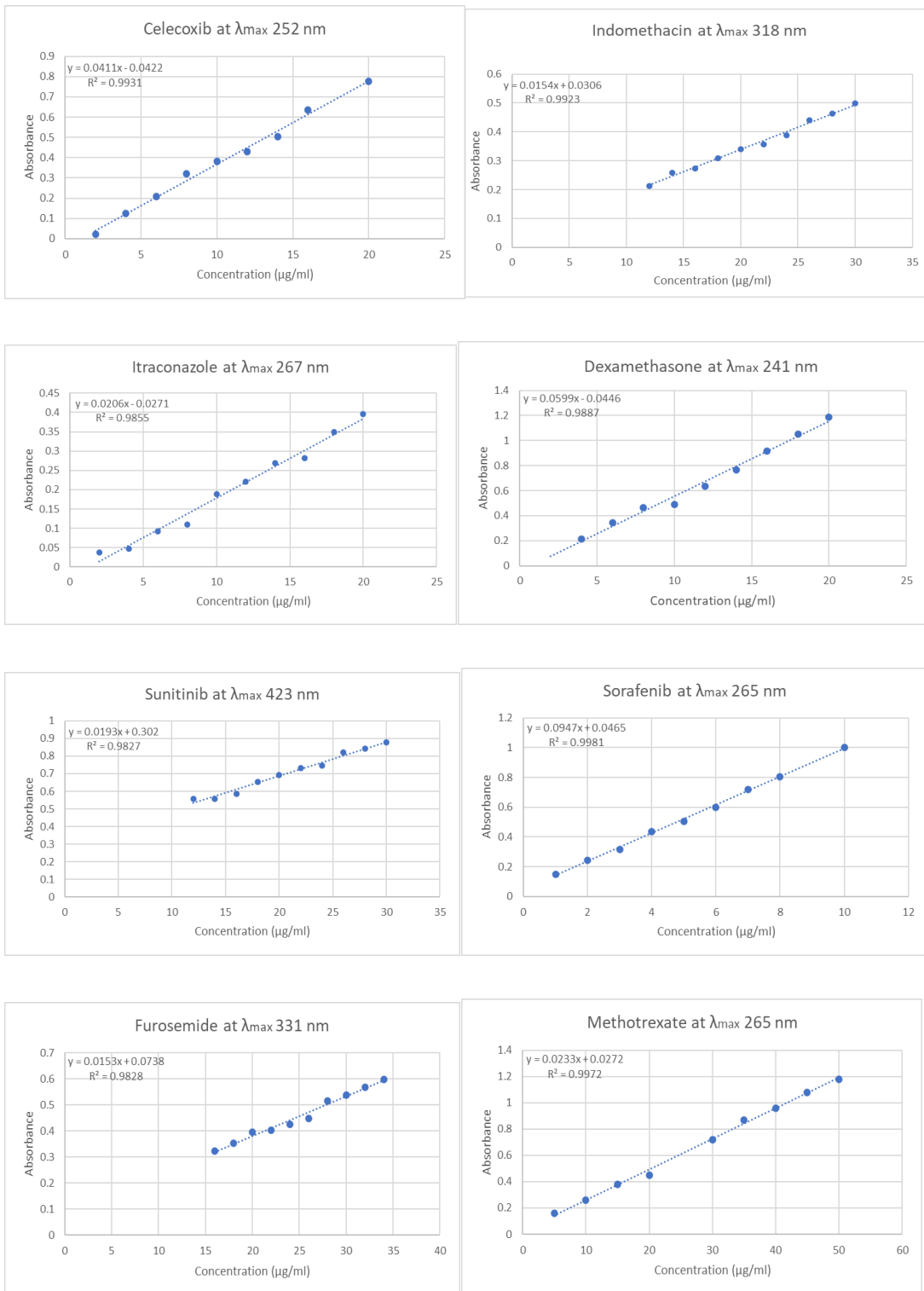


Figure 12. Calibration curves, regression equation and  $R^2$  value of all APIs using UV-Vis.

#### 4.4 Aqueous solubility of pure drugs

The aqueous solubility was determined using the same calibration curves as prepared for the determination of drug content in nanoemulsions and micelles. The solubility was calculated as the average of three samples per API. The water solubility values used in this study can be seen in Table IV. The aqueous solubility of dexamethasone, furosemide and methotrexate was significantly higher than for the other APIs.

Table IV. Calculated water solubilities of each API

API	Aqueous solubility ( $\mu\text{g/ml}$ )
Celecoxib	4.43
Indomethacin	6.84
Itraconazole	6.80
Dexamethasone	42.12
Sunitinib	6.72
Sorafenib	4.72
Furosemide	28.44
Methotrexate	65.44

#### 4.5 Polymer/surfactant ratio

In this study, the nanoemulsions were prepared using PDL as oil and mPEG-b-PDL as surfactant. In an earlier study, 1:6 (PDL:Kolliphor P 188) weight ratio was used at the fabrication of the nanoemulsions (Wik et al., 2019). Unfortunately, the cytotoxicity studies performed on cell culture showed, that higher concentrations of Kolliphor P 188 indicate higher cell mortality (Wik et al., 2019). Thereby, in this study, we aimed to use a minimum quantity of the surfactant resulting in a stable emulsion with a small size and polydispersity index (PDI). A ratio of 1:3 (PDL:mPEG-b-PDL) was found to be the minimum ratio to achieve a stable nanoemulsion. Compared to Kolliphor P 188, the same ratio failed to generate a stable nanoemulsion. This observation implies clearly that PDL has higher compatibility with mPEG-b-PDL than Kolliphor P 188. In Figure 13, the instability can be clearly seen, when a ratio of 1:2 was used. In addition, the effect of PDL (b and d) can be observed by decreasing the instability and formation of precipitation.

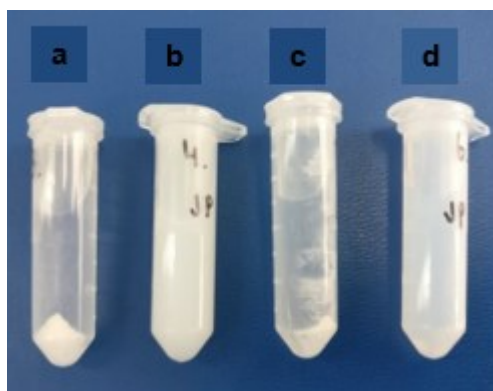


Figure 13. A picture of itraconazole nanoemulsions and micelles when 1:2 (PDL:mPEG-b-PDL) weight ratio was used. a) micelles with Kolliphor P 188, b) nanoemulsion with Kolliphor P 188, c) micelles with mPEG-b-PDL and d) nanoemulsion with mPEG-b-PDL. Instability can be clearly observed.

## 4.6 Characterization of nanoemulsions

### 4.6.1 Drug content

Since mPEG-b-PDL is capable of increasing the aqueous solubility of poorly soluble drugs, also mPEG-b-PDL micelles were prepared for all APIs for comparison. The aqueous solubility (Table IV) of the APIs was determined via the shake flask method and the results were utilized to calculate the increment in aqueous solubility for all APIs. The results can be seen in Figure 14. As expected based on the MD simulations, celecoxib gave the highest increment (~430 fold) and methotrexate the lowest (~10 fold). Thanks to the vital role of PDL encapsulation of the API, the solubility increments were considerably higher in nanoemulsions than in micelles. Dexamethasone was the only API deviating significantly from the MD-predicted order.

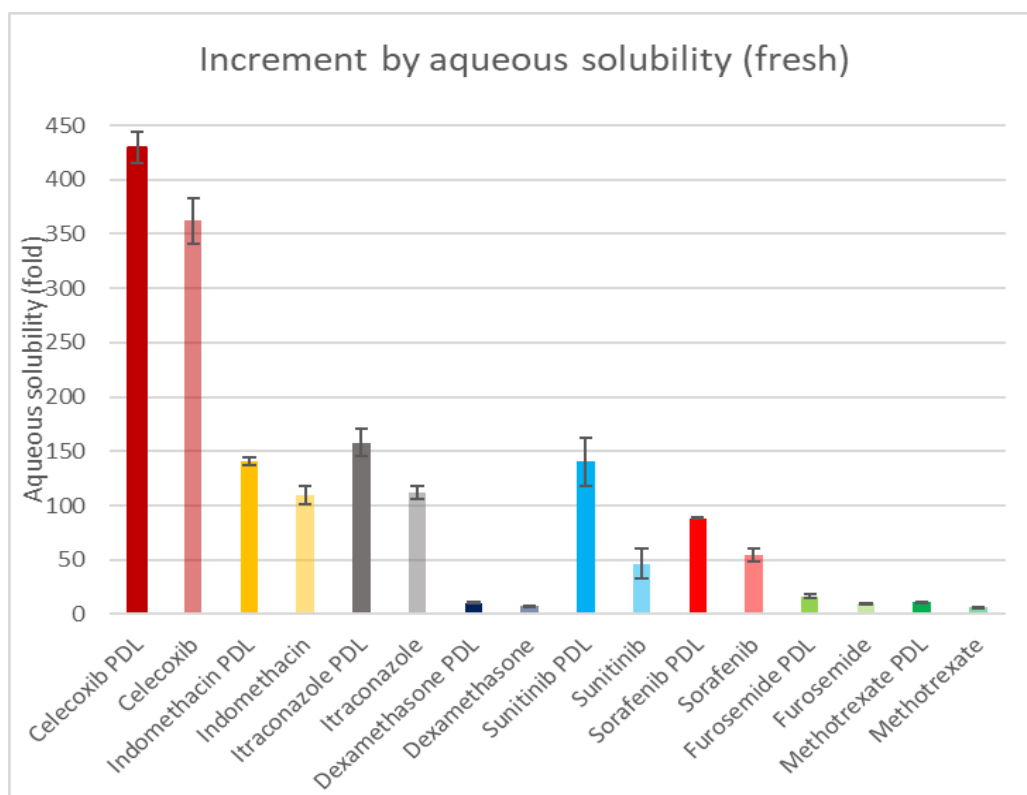


Figure 14. Increment in the aqueous solubility by fold of tested APIs using PDL nanoemulsion and mPEG-b-PDL micelles.

#### 4.6.2 Droplet size

The droplet size in the emulsion was analyzed by dynamic light scattering (DLS) as described in section 3.2.11. As presented in Table V, the mean hydrodynamic sizes by intensity ( $d$ , nm) (Figure 15) in the nanoemulsions were between 61.19 and 118.4 nm (SD 0.49-6.12) in the first peak. In turn, for the micelles, the mean hydrodynamic sizes laid between 42.45 and 61.86 nm (SD 0.95–5.00). It can be clearly seen that the PDL increased the droplet size 1.5-2-fold in nanoemulsions compared with the micelles due to PDL in the core. The PDL also increased the droplet size the closer the Hildebrand solubility parameter of the API was to the PDL. To be taken into consideration, the agitator speed, feed rate and temperature have shown to have a linear impact on the Z-average ( $d$ , nm) and size uniformity during fabrication (Oh et al., 2011).

Dexamethasone, sorafenib, furosemide and methotrexate gave a second peak in the size distribution in nanoemulsions, while all APIs in micelles expressed a second peak (Figure 15 for micelles), a so-called tail, which can be explained with aggregates in very small quantity. However, the second peak disappeared when the intensity distribution plot was converted to volume distribution. The polydispersity indexes in nanoemulsions varied between 0.133 and 0.25 (SD 0.0006–0.006) and between 0.219 and 0.323 (SD 0.004–0.032) in micelles. The PDI was slightly lower in nanoemulsions than micelles, indicating that the stabilizer increased homogeneity and lowered the risk of aggregation by disappearing the tail. In general, a PDI below 0.2 is considered acceptable and that was better achieved in nanoemulsions.

Table V. Mean droplet size by intensity ( $d$ , nm) and PDI with standard deviations (SD) in nanoemulsions and micelles

API	Nanoemulsion			Micelles		
	Peak 1 [SD]	Peak 2 [SD]	PDI [SD]	Peak 1 [SD]	Peak 2 [SD]	PDI [SD]
Celecoxib	118.4 [6.12]	-	0.25 [0.008]	47.58 [1.30]	569.2 [115.1]	0.244 [0.004]
Indomethacin	105.2 [0.87]	-	0.177 [0.014]	49.53 [5.00]	3314.7 [1310.8]	0.267 [0.007]
Itraconazole	119.6 [4.46]	-	0.248 [0.0006]	61.86 [1.28]	4979.3 [284.3]	0.323 [0.005]
Dexamethasone	61.19 [1.12]	4792 [33.94]	0.15 [0.016]	44.66 [3.90]	3084.7 [1028.3]	0.26 [0.032]
Sunitinib	73.69 [1.18]	-	0.133 [0.016]	60.17 [3.36]	4757 [427]	0.247 [0.032]
Sorafenib	73.62 [1.04]	3283.7 [1056.1]	0.219 [0.006]	59.31 [0.95]	4589 [100.2]	0.219 [0.008]
Furosemide	63.38 [0.58]	4978.5 [20.51]	0.139 [0.006]	42.45 [2.72]	919 [58.05]	0.296 [0.019]
Methotrexate	81.13 [0.49]	3571 [128.7]	0.232 [0.019]	49.52 [3.48]	2371.3 [1089.5]	0.251 [0.013]



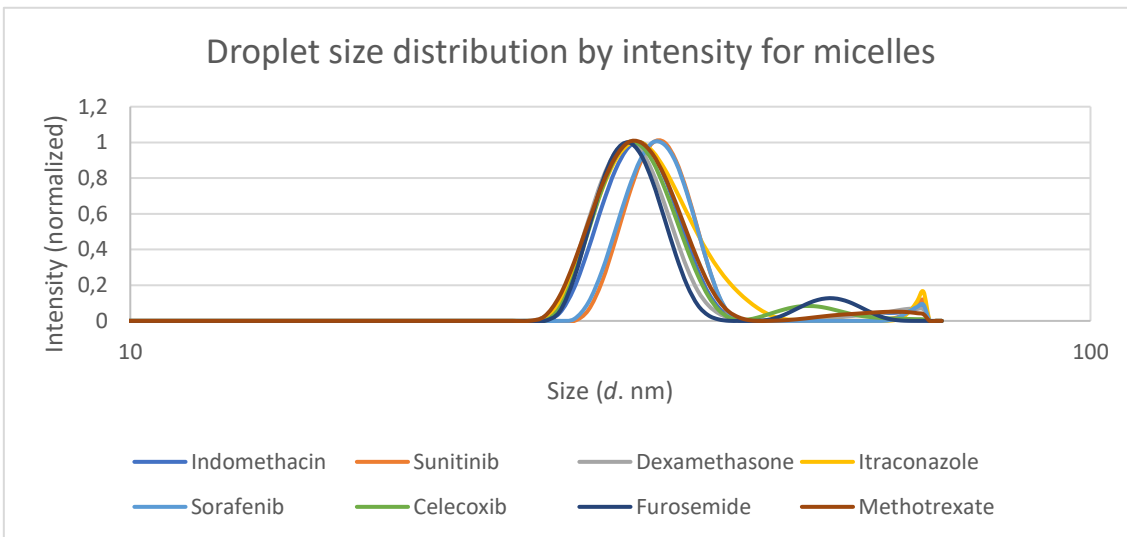
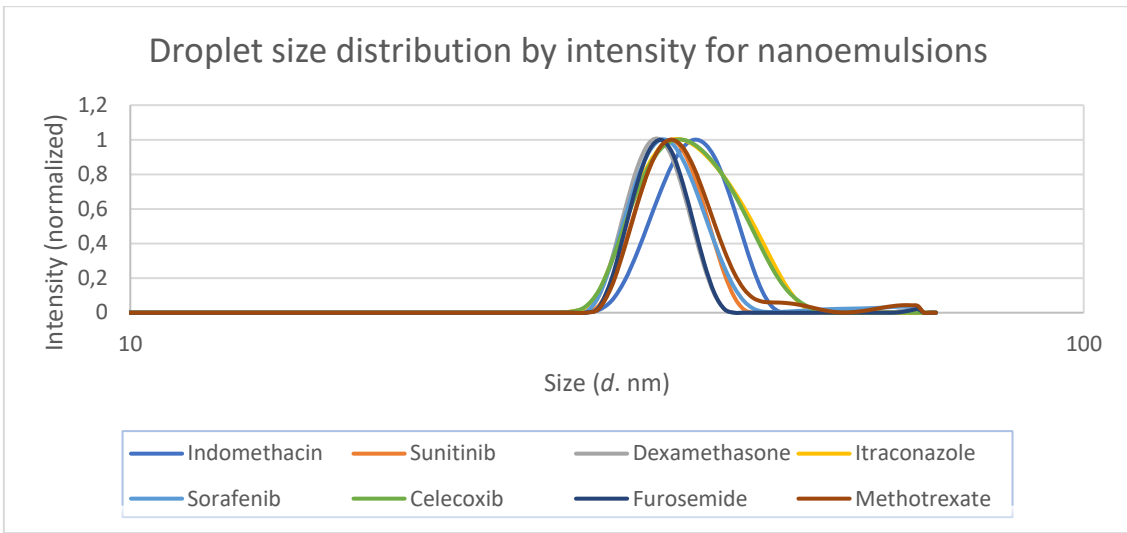


Figure 15. Droplet size distribution by intensity (normalized) for all eight APIs in nanoemulsion and micelles.

### 4.6.3 Stability

A visual stability check was performed by centrifuging the formulation at 13,500 RPM for 30 min to inspect possible separation or breaking. As shown in Figure 16, no signs of breaking, such as creaming, sedimentation or Ostwald ripening, were observed, which indicates good formulation stability (Bhatt et al., 2011).

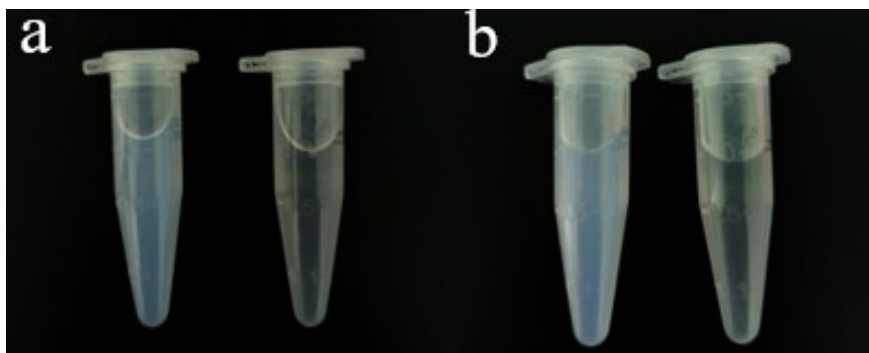


Figure 16. Pictures of nanoemulsion (hazy) and micelles (translucent) containing celecoxib a) before and b) after centrifugation at 13,500 RPM for 30 min.

The formulations were stored for 2 months at room temperature for size and drug content analysis. The analyses were performed every 30 days. No significant difference was observed in drug content within 2 months in the nanoemulsions. However, a tiny variation in size was observed in the micelles over time. As shown in Figure 17, the nanoemulsions and micelles, except with celecoxib, were placed in the same order by absorbance in the long-term study. Overall, the absorbances were 0.1–0.3 lower in micelles than nanoemulsions, which indicates lower concentrations of drug and appreciable effect of the PDL polymer.

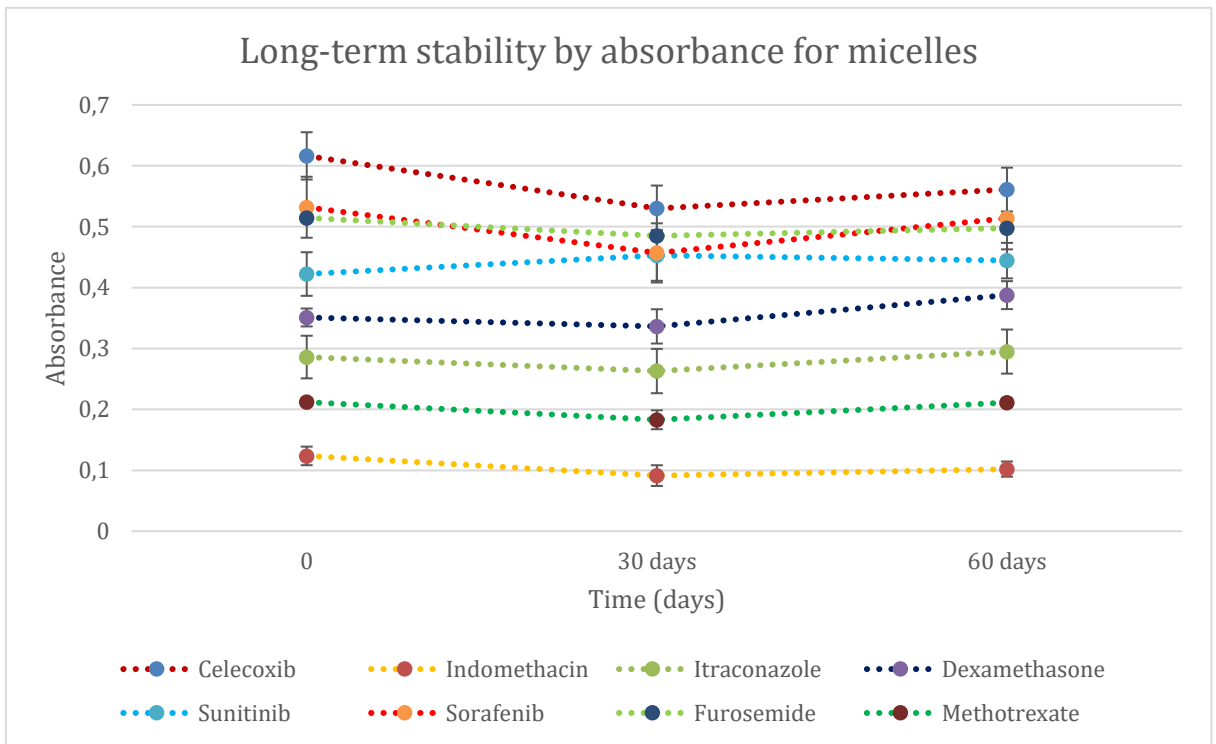
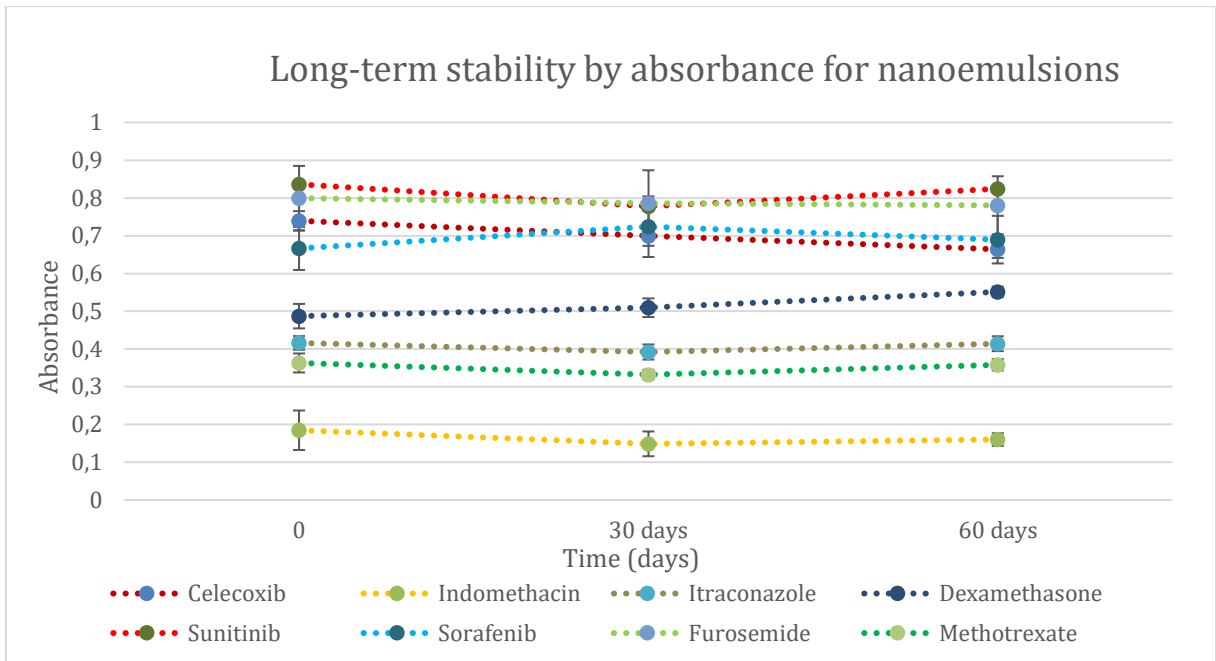


Figure 17. Drug content by absorbance for nanoemulsions and micelles, stored at room temperature for 60 days.

As shown in Figure 18, the change in Z-average size over time is evident. Sorafenib and methotrexate showed the highest stability by size, and the rest showed slight variability. The PDI was remarkably high at some APIs in measurements at 60 days but still, the Z-average size of nanoemulsion droplets and micelles remained below 100 nm. The findings imply that both nanoemulsions and micelles have good stability and can preserve drugs against degradation for at least two months.

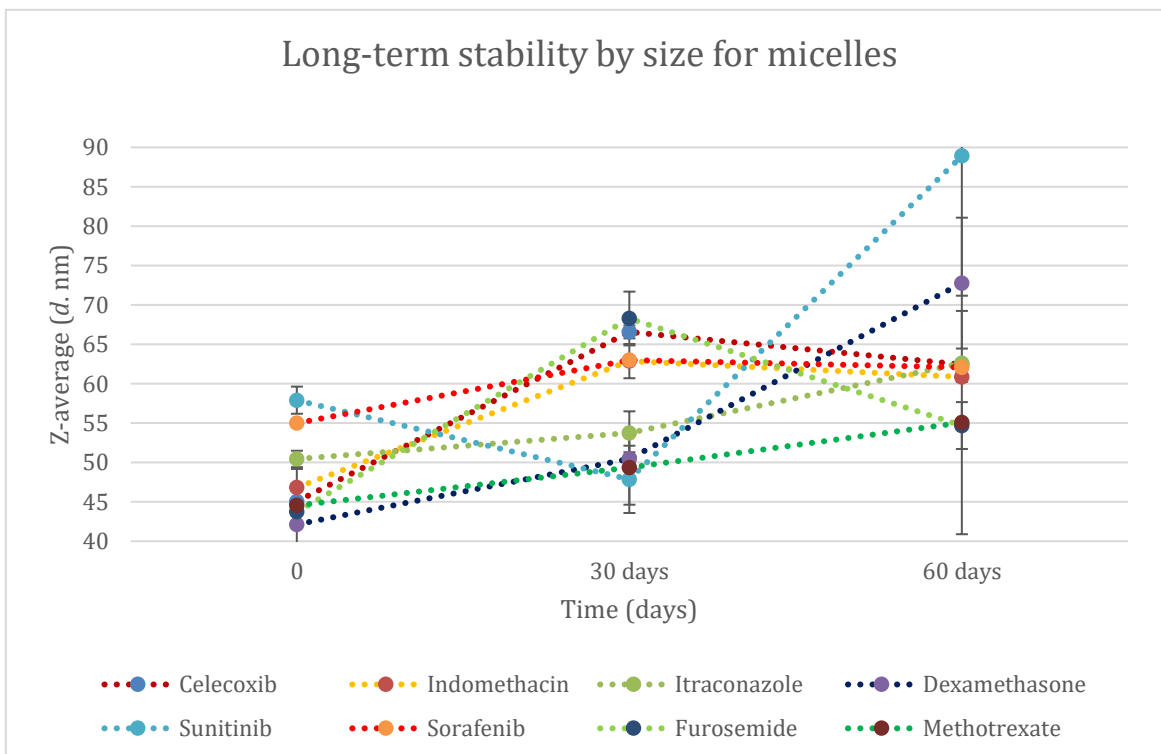
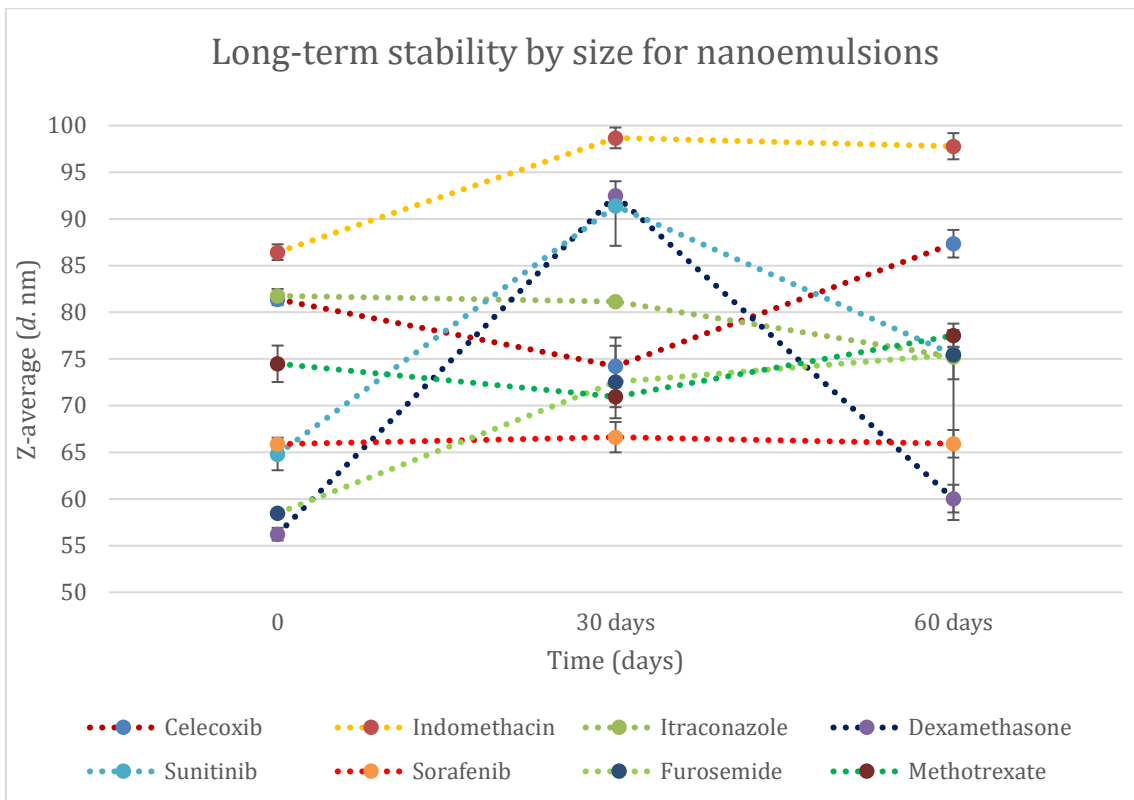


Figure 18. Stability by size (Z-average) over time for nanoemulsions and micelles, stored at room temperature for 60 days.

## 5 Discussion

Over time, there have been many investigations and approaches to overcome the challenge of poor aqueous solubility, such as particle size reduction, salt formation and the use of surfactants. Poor aqueous solubility indicates low bioavailability and lack of efficacy, being the biggest reason to hinder the drug molecule from reaching the market (Sareen et al., 2012). Therefore, in this project, a combination of two strategies, i.e., employing a polymeric surfactant and applying MD simulations for predicting drug-polymer miscibility, was proposed in order to generate a stable O/W nanoemulsion with high drug loading and increased aqueous solubility.

The first step in this study was to find APIs with  $\log P$  values between 1 and 5 and a poor aqueous solubility less than 0.1 mg/ml. The main source for the search was the PubChem database. For some APIs, it was more difficult to find reliable data than for the others, but in this step, directional data sufficed. The MD simulations were performed for homopolymer PDL, copolymer m-PEG-b-PDL and the APIs. Finally, the MDS results were observed and interpreted. Hildebrand solubility parameters played a key role in the selection of the APIs.

The MD-predicted miscibilities were later found to be consistent with the experimental values. However, there were two APIs that deviated from the MD-predicted miscibility order. Indomethacin and dexamethasone did not follow the expected order. This might be due to the fact that some of the APIs were taken from old stocks, hence they may have got degraded (Briscoe et al., 2009). Hence, the prediction of the miscibility between an oily polymer and API with the aid of MDS could help decrease the number of needed long-term experiments and costs as the conventional drug development process requires at least ten years. (Subashini et al., 2011)

Table II presents the Hildebrand solubility parameters and  $D_H$ . Forster et al. (2001) reported, that at the difference of  $<7.0 \text{ MPa}^{1/2}$  substances show significant miscibility and at difference  $>10 \text{ MPa}^{1/2}$  immiscibility. Furosemide and methotrexate had a  $D_H$  clearly higher than 10, and the increment of water solubility was clearly the lowest (Figure 14). The results in this study were supported better by the theory by Forster et al. (2001) than Venkatram et al. (2019). Also, the study by Stipa et al. (2021) supported our findings that there is an affiliation between the solubility increment and  $\log P$  value.  $\log P$  values close to 0 or below indicate that the API does not remain in the core of an oily polymer.

The droplet size for nanoemulsions and micelles was good, and a clear difference caused by PDL polymer was seen as expected. The APIs with higher concentrations and increments in solubility indicated larger droplet sizes. Still, the droplet sizes were clearly inside the range (20-200 nm) that is considered as the ideal range for stable nanoemulsions (Najahi-Missaoui et al., 2020; Jaiswal et al., 2015). However, small variation in the droplet sizes was observed, which could be caused by the manufacturing process of the nanoemulsions and micelles. Agitation speed, feed rate and sonication time in the droplet formation may have an influence on the droplet size (Oh et al., 2011).

Long-term stability showed no signs of breaking, such as coalescence, sedimentation or Ostwald ripening. The pictures before and after were uniform, indicating excellent formulation stability for at least two months (Bhatt et al., 2011; Tadros et al., 2004). Drug content in nanoemulsions and micelles was very stable for two months. As expected, nanoemulsions had higher drug concentrations than micelles thanks to the PDL polymer. Z-average by size showed a slight increase in droplet size in micelles suggesting agglomeration and weaker stability for some APIs. Nanoemulsions showed good stability for most of the APIs. For further investigation of the nanoemulsions, some essential parameters, such as pH, zeta potential and viscosity could be evaluated. Earlier studies have shown that PDL polymer and mPEG-b-PDL do not induce cell toxicity *in vitro* (Bansal et al., 2015; Wik et al., 2019). However, PDL nanoemulsions have shown time and concentration-dependent cell toxicity, suggesting that further toxicological studies of nanoemulsion containing PDL and mPEG-b-PDL (Wik et al., 2019) are necessary.

As a conclusion, the results in this study fulfilled the hypothesis and the objectives were reached. We succeeded to predict the miscibility between hydrophobic drugs and PDL polymer by using MDS. In addition, we developed a promising polymeric nanoemulsion formulation with high stability and encapsulation efficiency. The stability was achieved together with the aid of the PDL polymer and an in-house-made surfactant. Solubility is at the heart of pharmaceutical research and in this project, the PDL polymer showed its potential to increase the aqueous solubility of poorly soluble drugs. Finally, the in-house-made surfactant was shown to be efficient in smaller quantities than the commercial surfactant Kolliphor P 188.

## 6 Conclusion

In this work, MD simulations were employed to assess API miscibility with an oily polymer. The PDL polymer was selected as carrier to show its potential to increase the aqueous solubility of poorly soluble APIs. To forecast the miscibility of the drug molecules with PDL and the copolymer mPEG-b-PDL, we utilized the Hildebrand solubility parameter and Hildebrand distance ( $D_H$ ). mPEG-b-PDL was used as a surfactant in the nanoemulsions and independently as micelles in the experimental assessment. The increase in the aqueous solubility of the drugs in PDL nanoemulsion or mPEG-b-PDL micelles followed the MD-predicted miscibility trend supporting our computational findings. In comparison to the commercially available Kolliphor P 188, the PDL nanoemulsions were successfully stabilized by using mPEG-b-PDL as a stabilizer at a low concentration. Our findings also imply that combining a homopolymer with a copolymer in nanoformulation design could result in enhanced drug loading and less aggregate formation. The formulations were determined to be stable at room temperature for at least two months.

The results of this study suggest that MDS can be used as a rapid method to determine the most compatible and suitable drugs for the PDL polymer. The nanoemulsions using the PDL polymer then provide a potential approach to overcome the problem of poorly soluble drugs. The capability of the in-house-made block copolymer surfactant for stabilization was assessed, which proved its efficacy and opened a new direction for preparation of polymeric biphasic systems. The capability of the surfactant provided an indication for future research about the role of polymer-polymer interaction and hydrophilic-lipophilic balance (HLB) value on emulsion stabilization.

As a result, we believe that using MDS to predict the miscibility of PDL and APIs to build nanoformulations with high drug load, could save a significant amount of time and costs. The findings in this study could possibly be applied to different polymeric systems as well. Based on these results it can be concluded, that we have a promising basis for further research. The first *in vivo* studies have already been performed with the celecoxib nanoemulsion from this project.



## 7 Summary in Swedish - Svensk sammanfattning

### **Tillverkning och karakterisering av poly(decylactone) nanoemulsioner för användning av skräddarsydda surfaktanter för leverans av hydrofoba läkemedel**

Leverans av nya läkemedelsmolekyler till kroppen är allmänt utmanande på grund av deras låga vattenlöslighet, vilket därmed påverkar biotillgängligheten och den farmakologiska responsen. Majoriteten av nya läkemedelsmolekyler är hydrofoba, dvs. icke-vattenlösliga, vilket betyder att molekylen måste till exempel modifieras fysiskt, kemiskt eller bulkmaterialen måste förminska i storlek för att nå bättre löslighet och effekt. (Kapourani et al., 2021; Chaudhary et al., 2012) Låg biotillgänglighet kan också bero på låg permeabilitet.

I denna studie utnyttjades nanoteknologi, närmare sagt nanoemulsioner för att uppnå förbättrad vattenlöslighet för en rad svårslösliga molekyler. Nanoemulsion är ett heterogent system som består av en oljefas och en vattenfas, som sedan stabiliseras med ett eller flera ytaktiva ämnen som kallas surfaktanter. Surfaktanternas uppgift är att hålla faserna i en suspension med små partiklar och att undvika agglomering. Inom nanoteknologi har nanoemulsioner bevisats förbättra vattenlösligheten samt förminska biverkningar och toxicitet med mera. Nanoemulsioner har mångsidiga egenskaper såsom stor ytarea som ökar biotillgängligheten och förbättrar den fysiska stabiliteten. Nanoemulsioner kan administreras via flera olika rutter, som oralt, topiskt, intranasalt, pulmonärt och intravenöst i flera olika dosformer såsom vätska, fast, kräm eller aerosol. (Sharma et al., 2010; Singh et al., 2017)

Molekyldynamisk simulering är en modern datorsimuleringsmetod för att studera makromolekylers interaktion, dynamik och energi. Molekyldynamiksimuleringen är en snabb och effektiv metod att förutse hur till exempel en läkemedelssubstans och polymer växelverkar. Med hjälp av molekyldynamiksimuleringar förkortas experimenttiden men framför allt förminska kostnaderna. (Stipa et al., 2019)

Syftet med detta labbprojekt var att utveckla en stabil nanoemulsion samt bevisa att Hildebrands löslighetsparameter som resultat från de molekyldynamiska simuleringarna kan pålitligt användas för att hitta de mest kompatibla läkemedelssubstanserna för en polymer. Åtta läkemedelssubstanser med låg vattenlöslighet valdes till detta projekt för att utveckla en stabil nanoemulsion och undersöka polymerens förmåga att öka lösligheten samt bevisa att den skräddarsydda surfaktanten är mer effektiv än den kommersiella surfaktanten Kolliphor P 188.

De åtta läkemedelssubstanserna var celecoxib, dexametason, furosemid, indometacin, itrakonazol, metotrexat, sorafenib och sunitinib.

Polymeren PDL syntetiserades från en monomer  $\delta$ -dekalakton via en ringöppningspolymerisation. Nanoemulsionerna framställdes genom att blanda läkemedel med lösningsmedlet aceton, poly(dekalakton)polymer (PDL) mer och surfaktant (som även var polymerbaserad), som sedan droppvis tillsattes till avjoniserat vatten som var på magnetomrörning. Proverna fick sedan stå under omrörning i minst tre timmar utan kork för att lösningsmedlet skulle avdunsta. De färdiga proverna filtrerades till slut, så att läkemedel som inte lösts upp avlägsnades. För att visa effekten av PDL, framställdes referenslösningar utan PDL och även lösningar med Kolliphor P 188 som jämförelse. Analyser för absorbans, storlek och stabilitet gjordes för samtliga nanoemulsioner och referenslösningar.

Nanoemulsionernas koncentration av läkemedel uppskattades genom att analysera utspädda prover med hjälp av ultraviolettspektroskopi (UV-Vis) och beräkna koncentrationerna utgående från tidigare framställda kalibreringskurvor. Nanoemulsionerna innehöll en betydligt högre koncentration läkemedel än de jämförande prover som inte innehöll PDL-polymer. Koncentrationsökningen för nanoemulsionerna var 10–430 gånger och 6–362 gånger för de jämförande lösningarna för de åtta läkemedel som användes i denna studie. Storleksfördelningen visade att majoriteten av nanopartiklarna var av en storlek kring 100 nm och de största enskilda partiklarna var upp till 5000 nm. Stabilitetsstudier utfördes genom att centrifugera ett nanoemulsionsprov och referensprov i 30 minuter och sedan visuellt bedöma resultatet. Ingen separering kunde upptäckas. Stabiliteten undersöktes även genom att förvara tre läkemedelsladdade nanoemulsioner i två månader i rumstemperatur ( $20 \pm 2$  °C). Under de två månaderna kunde inga trender utifrån resultaten för storleksfördelning observeras, ingen tydlig separering i nanoemulsionerna hade heller uppstått under denna tid. Detta tyder på att nanoemulsionerna är stabila åtminstone i två månaders tid.

Att använda PDL-polymeren för att framställa nanoemulsioner är ett relativt nytt tillvägagångssätt och därmed finns det få jämförelsedata tillgängliga. Resultaten av denna studie genererar en snabb validerad metod för att bestämma de mest kompatibla läkemedelssubstanserna för PDL-polymeren via molekylodynamiska simuleringar. Resultaten tyder också på att kombinationen av en homopolymer (PDL) och sampolymer (surfaktant) kan leda till en hög laddningsgrad samt minska bildningen av kluster.

## 8 References

- Abbott, S., & Hansen, C. M. (2008). *Hansen solubility parameters in practice*. Hansen-Solubility.
- Bansal, K. K., Kakde, D., Purdie, L., Irvine, D. J., Howdle, S. M., Mantovani, G., & Alexander, C. (2015). New biomaterials from renewable resources—amphiphilic block copolymers from  $\delta$ -decalactone. *Polymer chemistry*, 6(40), 7196-7210.
- Bibi, H. A., Holm, R., & Bauer-Brandl, A. (2017). Simultaneous lipolysis/permeation in vitro model, for the estimation of bioavailability of lipid based drug delivery systems. *European Journal of Pharmaceutics and Biopharmaceutics*, 117, 300-307.
- Binks, B. P. (2002). Particles as surfactants—similarities and differences. *Current opinion in colloid & interface science*, 7(1-2), 21-41.
- Bergström, C. A., Wassvik, C. M., Johansson, K., & Hubatsch, I. (2007). Poorly soluble marketed drugs display solvation limited solubility. *Journal of medicinal chemistry*, 50(23), 5858-5862.
- Bhatt, P., & Madhav, S. (2011). A detailed review on nanoemulsion drug delivery system. *International Journal of Pharmaceutical sciences and research*, 2(10), 2482.
- Briscoe, C. J., & Hage, D. S. (2009). Factors affecting the stability of drugs and drug metabolites in biological matrices.
- Bowers, K. J., Chow, D. E., Xu, H., Dror, R. O., Eastwood, M. P., Gregersen, B. A., ... & Shaw, D. E. (2006, November). Scalable algorithms for molecular dynamics simulations on commodity clusters. In *SC'06: Proceedings of the 2006 ACM/IEEE Conference on Supercomputing* (pp. 43-43). IEEE.
- Burke, J. (1984). Solubility parameters: theory and application.
- Calculate reagent log P values to determine solubility characteristics. *TECH TIP #56 Thermo Fischer*. (Retrieved on 23.9.2021 <https://assets.thermofisher.com/TFS-Assets/LSG/Application-Notes/TR0056-Calc-logP.pdf>)
- Chatterjee, B., Gorain, B., Mohananaidu, K., Sengupta, P., Mandal, U. K., & Choudhury, H. (2019). Targeted drug delivery to the brain via intranasal nanoemulsion: Available proof of concept and existing challenges. *International journal of pharmaceutics*, 565, 258-268.
- Chaudhary, A., Nagaich, U., Gulati, N., Sharma, V. K., Khosa, R. L., & Partapur, M. U. (2012). Enhancement of solubilization and bioavailability of poorly soluble drugs by physical and chemical modifications: A recent review. *J Adv Pharm Educ Res*, 2(1), 32-67.
- Chime, S. A., Kenekwku, F. C., & Attama, A. A. (2014). Nanoemulsions—advances in formulation, characterization and applications in drug delivery. *Application of nanotechnology in drug delivery*, 3, 77-126.

- Custodio, J. M., Wu, C. Y., & Benet, L. Z. (2008). Predicting drug disposition, absorption/elimination/transporter interplay and the role of food on drug absorption. *Advanced drug delivery reviews*, 60(6), 717-733.
- Forster, A., Hempenstall, J., & Rades, T. (2001). Characterization of glass solutions of poorly water-soluble drugs produced by melt extrusion with hydrophilic amorphous polymers. *Journal of Pharmacy and Pharmacology*, 53(3), 303-315.
- Hancock, B. C., York, P., & Rowe, R. C. (1997). The use of solubility parameters in pharmaceutical dosage form design. *International journal of pharmaceutics*, 148(1), 1-21.
- Hill, A. P., & Young, R. J. (2010). Getting physical in drug discovery: a contemporary perspective on solubility and hydrophobicity. *Drug discovery today*, 15(15-16), 648-655.
- Hossain, S., Kabelev, A., Parrow, A., Bergström, C., & Larsson, P. (2019). Molecular simulation as a computational pharmaceutics tool to predict drug solubility, solubilization processes and partitioning. *European Journal of Pharmaceutics and Biopharmaceutics*.
- Jaiswal, M., Dudhe, R., & Sharma, P. K. (2015). Nanoemulsion: an advanced mode of drug delivery system. *3 Biotech*, 5(2), 123-127.
- Kapourani, A., Eleftheriadou, K., Kontogiannopoulos, K. N., & Barmpalexis, P. (2021). Evaluation of rivaroxaban amorphous solid dispersions physical stability via molecular mobility studies and molecular simulations. *European Journal of Pharmaceutical Sciences*, 157, 105642.
- Katepalli, H. (2014). Formation and stability of emulsions: Effect of surfactant-particle interactions and particle shape.
- Kim, S., Chen, J., Cheng, T., Gindulyte, A., He, J., He, S., ... & Bolton, E. E. (2021). PubChem in 2021: new data content and improved web interfaces. *Nucleic acids research*, 49(D1), D1388-D1395.
- Krol, S. (2020). Therapeutic Benefits from Nanoparticles. *21st Century Nanoscience—A Handbook: Nanopharmaceutics, Nanomedicine, and Food Nanoscience (Volume Eight)*.
- Kumar, N., & Mandal, A. (2018). Surfactant stabilized oil-in-water nanoemulsion: stability, interfacial tension, and rheology study for enhanced oil recovery application. *Energy & Fuels*, 32(6), 6452-6466.
- Lau, E. (2001). Preformulation studies. *Handbook of modern pharmaceutical analysis*, 3, 173-224.
- Loureiro, J. A., & Pereira, M. C. (2020). PLGA based drug carrier and pharmaceutical applications: the most recent advances. *Pharmaceutics*, 12(9), 903.
- Mandal, Ananya. (2019, April 03). Safety of Nanoparticles. News-Medical. Retrieved on April 27, 2022 from <https://www.news-medical.net/life-sciences/Safety-of-Nanoparticles.aspx>.

- Murtaza, G., Khan, S. A., Najam-ul-Haq, M., & Hussain, I. (2014). Comparative evaluation of various solubility enhancement strategies for furosemide. *Pakistan Journal of Pharmaceutical Sciences*, 27(4).
- Najahi-Missaoui, W., Arnold, R. D., & Cummings, B. S. (2020). Safe nanoparticles: Are we there yet?. *International Journal of Molecular Sciences*, 22(1), 385.
- Nishitani Yukuyama, M., Tomiko Myiake Kato, E., Lobenberg, R., & Araci Bou-Chacra, N. (2017). Challenges and future prospects of nanoemulsion as a drug delivery system. *Current pharmaceutical design*, 23(3), 495-508.
- Nordin, U. U. M., Ahmad, N., Salim, N., & Yusof, N. S. M. (2021). Lipid-based nanoparticles for psoriasis treatment: a review on conventional treatments, recent works, and future prospects. *RSC Advances*, 11(46), 29080-29101.
- Oh, D. H., Balakrishnan, P., Oh, Y. K., Kim, D. D., Yong, C. S., & Choi, H. G. (2011). Effect of process parameters on nanoemulsion droplet size and distribution in SPG membrane emulsification. *International journal of pharmaceutics*, 404(1-2), 191-197.
- Ouyang, D., & Smith, S. C. (2015). Introduction to computational pharmaceutics. *Computational Pharmaceutics*, 1-5.
- Porter, C. J., Trevaskis, N. L., & Charman, W. N. (2007). Lipids and lipid-based formulations: optimizing the oral delivery of lipophilic drugs. *Nature reviews Drug discovery*, 6(3), 231-248.
- Profacgen. (n.d.). *Molecular dynamics simulation*. Retrieved on 27.5.2022 from [Mayhttps://www.profacgen.com/molecular-dynamics-simulation.htm](https://www.profacgen.com/molecular-dynamics-simulation.htm)
- Pyrhönen, J., Bansal, K. K., Bhadane, R., Wilén, C. E., Salo-Ahen, O. M., & Rosenholm, J. M. (2022). Molecular Dynamics Prediction Verified by Experimental Evaluation of the Solubility of Different Drugs in Poly (decalactone) for the Fabrication of Polymeric Nanoemulsions. *Advanced NanoBiomed Research*, 2(1), 2100072.
- Rog, T., & Bunker, A. (2020). Mechanistic understanding from molecular dynamics simulation in pharmaceutical research 1: drug delivery. *Frontiers in Molecular Biosciences*, 7, 371.
- Roos, K., Wu, C., Damm, W., Reboul, M., Stevenson, J. M., Lu, C., ... & Harder, E. D. (2019). OPLS3e: Extending force field coverage for drug-like small molecules. *Journal of chemical theory and computation*, 15(3), 1863-1874.
- Tayeb, H. H., & Sainsbury, F. (2018). Nanoemulsions in drug delivery: formulation to medical application. *Nanomedicine*, 13(19), 2507-2525.
- Salo-Ahen, O. M., Alanko, I., Bhadane, R., Bonvin, A. M., Honorato, R. V., Hossain, S., ... & Vanmeert, M. (2020). Molecular dynamics simulations in drug discovery and pharmaceutical development. *Processes*, 9(1), 71.
- Sareen, S., Mathew, G., & Joseph, L. (2012). Improvement in solubility of poor water-soluble drugs by solid dispersion. *International journal of pharmaceutical investigation*, 2(1), 12.

- Shafiq, S., Shakeel, F., Talegaonkar, S., Ahmad, F. J., Khar, R. K., & Ali, M. (2007). Development and bioavailability assessment of ramipril nanoemulsion formulation. *European journal of pharmaceutics and biopharmaceutics*, 66(2), 227-243.
- Sharma, N., Bansal, M., Visht, S., Sharma, P. K., & Kulkarni, G. T. (2010). Nanoemulsion: A new concept of delivery system. *Chronicles of Young Scientists*, 1(2), 2.
- Shreya, A. B., Raut, S. Y., Managuli, R. S., Udupa, N., & Mutalik, S. (2019). Active targeting of drugs and bioactive molecules via oral administration by ligand-conjugated lipidic nanocarriers: recent advances. *AAPS PharmSciTech*, 20(1), 1-12.
- Shu, G., Khalid, N., Zhao, Y., Neves, M. A., Kobayashi, I., & Nakajima, M. (2016). Formulation and stability assessment of ergocalciferol loaded oil-in-water nanoemulsions: Insights of emulsifiers effect on stabilization mechanism. *Food research international*, 90, 320-327.
- Singh, Y., Meher, J. G., Raval, K., Khan, F. A., Chaurasia, M., Jain, N. K., & Chourasia, M. K. (2017). Nanoemulsion: Concepts, development and applications in drug delivery. *Journal of controlled release*, 252, 28-49.
- Solans, C., Izquierdo, P., Nolla, J., Azemar, N., & Garcia-Celma, M. J. (2005). Nanoemulsions. *Current opinion in colloid & interface science*, 10(3-4), 102-110.
- Sonneville-Aubrun, O., Simonnet, J. T., & L'aloret, F. (2004). Nanoemulsions: a new vehicle for skincare products. *Advances in colloid and interface science*, 108, 145-149.
- Stipa, P., Marano, S., Galeazzi, R., Minnelli, C., Mobbili, G., & Laudadio, E. (2021). Prediction of drug-carrier interactions of PLA and PLGA drug-loaded nanoparticles by molecular dynamics simulations. *European Polymer Journal*, 147, 110292.
- Subashini, M., Devarajan, P. V., Sonavane, G. S., & Doble, M. (2011). Molecular dynamics simulation of drug uptake by polymer. *Journal of Molecular Modeling*, 17(5), 1141-1147.
- Tadros, T. F. (2003). Surfactants, industrial applications.
- Tadros, T. F., Vandamme, A., Leveck, B., Booten, K., & Stevens, C. V. (2004). Stabilization of emulsions using polymeric surfactants based on inulin. *Advances in colloid and interface science*, 108, 207-226.
- Tadros, T. F. (Ed.). (2013). *Emulsion formation and stability*. John Wiley & Sons, Incorporated. (11.1.22, 16.1.22)
- Venkatram, S., Kim, C., Chandrasekaran, A., & Ramprasad, R. (2019). Critical assessment of the Hildebrand and Hansen solubility parameters for polymers. *Journal of chemical information and modeling*, 59(10), 4188-4194.
- Weerachanchai, P., Wong, Y., Lim, K. H., Tan, T. T. Y., & Lee, J. M. (2014). Determination of solubility parameters of ionic liquids and ionic liquid/solvent mixtures from intrinsic viscosity. *ChemPhysChem*, 15(16), 3580-3591.

Wik, J., Bansal, K. K., Assmuth, T., Rosling, A., & Rosenholm, J. M. (2019). Facile methodology of nanoemulsion preparation using oily polymer for the delivery of poorly soluble drugs. *Drug Delivery and Translational Research*, 1-13.

Zhang, X., Xing, H., Zhao, Y., & Ma, Z. (2018). Pharmaceutical dispersion techniques for dissolution and bioavailability enhancement of poorly water-soluble drugs. *Pharmaceutics*, 10(3), 74.